Earthquake Research at Parkfield

April 5, 2001

Draft

Summary

The USGS and its collaborators have intensively monitored seismicity, crustal deformation, and electromagnetic properties along the Parkfield segment of the San Andreas fault since the mid-1980's in the hope of recording the details of strain accumulation prior to a $M6$ earthquake as well as of seismic rupture propagation. The earthquake was expected before 1993, but has not occurred. Current estimates of the likelihood of the next Parkfield earthquake are about 10%/year.

Even without having a $M6$ mainshock, the Parkfield data set already acquired addresses several fundamental issues of earthquake physics with direct implications for hazard assessment: the validity of strain-budget balancing, the variability of recurrence intervals, the role of fault trace discontinuities in defining fault segments that can rupture in a single earthquake, the physical linkage of foreshocks to a mainshock, and the synthesis of realistic ground-motion time histories. Parkfield data are in principle available to the scientific community and the process of placing them in internet-accessible archives is well along.

Near-field data before and during a $M6$ earthquake at Parkfield should provide valuable constraints on fault constitutive laws used in numerical models for faulting. These constraints yield insights into the physics of earthquakes and might be used in short or intermediate term forecasts of future earthquakes that are based upon physics rather than the empirical relationships that are currently being used.

A moderate Parkfield earthquake will also provide high-quality, near-field recordings of high-frequency seismic ground motions that will allow delineation of the propagating rupture front. This detailed information will help researchers provide realistic ground motion time histories for engineering purposes.

Future plans for Parkfield include two NSF initiatives, the San Andreas Fault Observatory at Depth (SAFOD) and the Plate Boundary Observatory (PBO). The major component of SAFOD is logging and instrumenting a 4 km deep borehole into the fault at Parkfield. This will provide valuable data on the in-situ physical properties of the fault zone at seismogenic depths. One component of PBO is to expand the existing set of instrumentation currently at Parkfield to address several long-standing issues on strain accumulation and seismic and aseismic release of energy along the Plate boundary.

In FY2000, the total cost of activities at Parkfield was $1.15M. The USGS Earthquake Hazards Program spent $600K to support ongoing monitoring at Parkfield, and NSF provided $75K support. Total USGS cost for all Parkfield activities, including studies and upgrades in support of SAFOD, was $757K in FY2000.

We recommend that the Parkfield experiment be continued and enhanced. Many of the instruments producing the most valuable data are near the end of their expected lifetimes or rely upon dated, difficult-to-maintain technology. Other instruments do not produce useful data and can be decommissioned. The estimated cost of these adjustments is $540K. Continued operation of the experiment at that level can be expected to approximate FY2000 levels.

Brief History of Parkfield Experiment

The Parkfield earthquake research program is an effort to understand earthquake physics through study of instrumental measurements along the San Andreas fault section with the highest known probability of generating a $M6$ earthquake in the next three decades. A secondary goal is to detect any anomalies of seismicity, ground deformation, or other physical quantities that might be premonitory to earthquakes in the Parkfield area. Improved knowledge of earthquake generation mechanisms will provide a scientific basis for refining estimates of future times, locations, magnitudes, and ground shaking of damaging earthquakes, not only at Parkfield, but also in more populated areas.

Since the Parkfield experiment began in 1985, earthquakes elsewhere in California have caused deaths, injuries, and huge economic losses. Obviously, it would have been beneficial if Parkfield-like data could have been acquired prior to these earthquakes. Unfortunately, a Parkfield-style experiment is possible only where the earthquake's nucleation point is believed known within about a 10-km radius. Consequently, while instruments of the types deployed at Parkfield now also operate in the San Francisco Bay Area and Los Angeles basin, their distribution is too sparse to record aseismic deformation and strong motion well enough to advance our fundamental understanding of earthquake nucleation and rupture propagation. Only at Parkfield is there enough information to focus adequate instrumentation exactly where the earthquake is likely to start. Worldwide, only the Tokai earthquake gap program in Japan approaches Parkfield in density of instrumentation near the source of a potential moderate-sized earthquake.

Instrumentation in the Parkfield area was sparse before 1984, and installation of many additional instruments did not seem justified until *Bakun and McEvilly* [1979] and *Bakun and Lindh* [1985] showed that similar $M \sim 6$ earthquakes in 1857, 1881, 1901, 1922, 1934, and 1966 likely occurred at almost the same location. *Bakun and Lindh* [1985] calculated an average repeat time of 22 years and a 95% confidence that a $M6$ earthquake would occur before 1993 near the site of the 1966 $M6$ earthquake (Figure 1). *Bakun and Lindh* [1985] also pointed out that the 1934 and 1966 earthquakes had similar epicenters, fault-plane solutions, and seismograms, and that both ruptures propagated southeastward. Moreover, in both 1934 and 1966, a $M5$ foreshock preceded the mainshock by 17 minutes, and these

two foreshocks also generated similar seismograms. These reasons to anticipate a future $M6$ earthquake nucleating near the same point in Parkfield were supplemented by geodetic data indicating that the Parkfield fault segment was accumulating strain rapidly enough togenerate another $M6$ earthquake before 1993 [*Segall and Harris*, 1987; *Harris and Segall*, 1987].

In response to these observations, the Parkfield Earthquake Prediction Experiment [*Bakun et. al.*, 1987] was created to add instruments to measure physical properties prior to, during, and after the anticipated earthquake. The USGS has collaborated with the State of California, University of California at Berkeley, the Commonwealth Scientific and Industrial Research Organization (CSIRO) of Australia, Stanford University, and the University of California at Riverside to measure and monitor a variety of physical parameters at Parkfield. Projects have included short-term experiments (e.g., seismic refraction, seismic reflection, and magneto-telluric surveys), as well as long-term monitoring of aseismic fault slip using creepmeters and electronic distance meters (EDM), aseismic deformation using strainmeters and water wells, electromagnetic field in a variety of frequency bands, and detailed recording of local earthquakes. Most USGS efforts have been tied to the long-term measurements. The locations of the instruments used in these long-term studies are shown in Figure 1 and Table 1.

Alert threshold levels, representing estimated probabilities of a M6 event in a 72-hour window, were developed for several types of instruments. For seismicity, alerts were generated for earthquakes sufficiently large and close to the 1966 hypocenter, with probabilities inferred from the foreshock histories of past Parkfield earthquakes. For fault creep, alert levels were set at creep rates higher than any previously observed at Parkfield. For magnetometers, strainmeters, and water-level sensors, no data were available for earlier Parkfield earthquakes, so the alert thresholds were simply based on the observed variability of the data record. For the levels that corresponded to significant likelyhood (¿10%) of a $M6$ event in a 72-hour window, the USGS would alert the California Office of Emergency Services of the potential of a geologic hazard.

By 1992, no $M6$ event had occurred, and the *NEPEC Working Group* [1994] attributed the failed prediction to inadequate physical theory and statistical models. The Working Group also concluded that the $M6$ might still be imminent. As it turned out, the $M6$ was even then not imminent, and the Bakun-Lindh prediction remains unfulfilled two years beyond the maximum known repose interval of 32 years. While the statistical analysis of past Parkfield recurrence intervals has been widely criticized, the similarities of past $M6$ sequences are still viewed as significant, and the analyses of strain accumulation rates have been updated and shown to still be valid.

Despite the overdue earthquake, the Parkfield section of the San Andreas fault is arguably the best location in the nation for concentrated study, based on its past short recurrence intervals, and apparent mechanical simplicity. Moreover, the lack of an earthquake early in the measurement program actually has benefits. Had the earthquake occurred early in the experiment, the data record would have been too short to fully quantify any temporal changes prior to the earthquake. As it is, some data records, if continued, will

span a large fraction of the present earthquake cycle. Recent advances in instrument sensitivity and deployment density should provide better constraints on physical theory of earthquakes and better resolution of any premonitory signals. Finally, two proposed NSF programs, the San Andreas Fault Observatory at Depth (SAFOD) and the Plate Boundary Observatory (PBO), would provide new information on earthquake nucleation, seismic rupture, and the overall earthquake cycle at Parkfield.

The SAFOD initiative [*Zoback et al.,* 1998] proposes to drill 4 km to penetrate and sample the San Andreas fault just north of the 1966 $M6$ nucleation point. Downhole logging and geophysical experiments will determine physical properties of the fault zone as it undergoes small repeating earthquakes as well as aseismic creep. The relatively shallow instrumentation currently at Parkfield provides a context for SAFOD's examination of the physics of faulting at depth. The Parkfield experiment could be altered to better complement SAFOD by deploying more geodetic instrumentation near the anticipated $M6$ nucleation zone.

In contrast to the single-borehole focus of SAFOD, the PBO experiment will examine the mechanics of faulting (and volcanism) on a regional scale, distributing new Global Positioning System (GPS) stations and borehole strainmeters broadly along the boundary between the Pacific plate and its adjoining plates from Southern California to Alaska. Most of these sensors will be deployed in clusters that target specific tectonic problems in detail and with some instrumental redundancy. The USGS experiment at Parkfield can be viewed as a PBO prototype which has already accumulated 15 years of data from strainmeters and other crustal deformation instruments. Parkfield's selection as a PBO cluster indicates that the research community broadly supports continuing and enhancing this research project.

In FY2000, \$1.15M was spent at Parkfield to support monitoring, SAFOD site studies, instruments enhancements, and modeling (Figure 2). Of that total, the USGS share is 66%. Monitoring activities constitute 52% of the total Parkfield expenses. Most of the USGS contribution is salary support, which is 60% of the cost of monitoring.

Here, we review the scientific results of the Parkfield program and point out unresolved issues that can be investigated by continuing and enhancing the experiment. Although it was believed originally that the experiment would last only a few years, we argue that this experiment's duration should span an earthquake recurrence interval. Parkfield still represents a unique opportunity to better understand earthquake mechanics. The instrumentation needs to be upgraded and enhanced to take advantage of new technology and to operate efficiently, and to that end we present recommendations for future allocation of resources.

Research Results and Future Opportunities

Even before observing the anticipated $M6$ event, the Parkfield Experiment has yielded data providing insight into recurrence models and the relation between strain accumulation

and its eventual release in earthquakes. One outstanding feature of the Parkfield Experiment is the acquisition of a detailed geodetic dataset documenting aseismic fault processes, which do not radiate seismic waves and can therefore only be detected using instruments placed close to the source. Microearthquake recording at Parkfield is also unmatched in its sensitivity and resolution. These observations have stimulated new research questions in our quest to understand earthquake mechanics and the seismic cycle.

Forecasting the Next Parkfield Earthquake

There are three methods for estimating the time of the next $M6$ based on lengths of previous $M6$ earthquake cycles at Parkfield and on geodetic data. The two methods discussed here make little use of mechanical principles and none of time-varying or premonitory deformation. In constrast, a third method, which uses both fault mechanics and deformation data, is discussed in a later section.

1. Statistical Analysis of Past Recurrence Intervals

The forecast with a 95% confidence that a $M6$ earthquake would occur near Parkfield before 1993 was based on extrapolation of an average 22-year period between moderate-sized earthquakes at Parkfield since 1857. This calculation [*Bakun and Lindh*, 1985] did not incorporate the real variability in earthquake recurrence intervals: Parkfield's recurrence intervals have been as short as 12 years, and as long as 34 years.

Paleoseismology has discovered similar variability in recurrence intervals at the sites of great earthquakes, such as southern California and Cascadia. Newer statistical models that more accurately reflect this variability yield an annual earthquake probability for a $M \geq 6$ at Parkfield of roughly 10% [*NEPEC Working Group,* 1994].

At present, earthquake probability calculations simply include variability of recurrence intervals as a statistical parameter because the reasons why earthquake recurrence intervals on a single fault segment can vary by a factor of three are unknown. At Parkfield, a long, detailed record of geodetic data offers clues to factors affecting the lengths of individual inter-earthquake repose intervals. The two most recent Parkfield recurrence intervals were 12 years (1922-1934) and 32 years (1934-1966). *Segall and Du* [1993] compared coseismic displacements for the 1934 and 1966 earthquakes and found that the 1966 earthquake ruptured through a fault stepover that had apparently arrested the 1934 earthquake. Additional strain energy accumulated during the longer repose interval between the 1934 and the 1966 events may have enabled the latter event to propagate further, perhaps as postseismic slip. Also, the nearby $M6.7$ Coalinga earthquake in 1983 temporarily changed strain accumulation rates at Parkfield, as indicated by creep and microseismicity rates.

The current Parkfield repose interval – the longest since 1857 –can be expected to yield more information about why recurrence intervals vary, which will in turn allow more accurate earthquake probability estimates to be made.

2. Conservation of strain energy

Another approach to earthquake forecasting is based on the idea that an earthquake releases stored strain energy that has gradually been accumulated during the preceding period of repose. In practice, this strain energy budget balance is carried out in terms of fault slip and is termed the "slip-predictable" recurrence model. The amount of slip in past earthquakes is estimated using paleoseismic techniques, the rate at which slip deficit is accumulating is estimated from contemporary geodetic measurements, and the expected recurrence interval is then obtained as the quotient. Although our best present probability estimates utilize this methodology, Parkfield is the only place where it can be rigorously tested. The outcome of the test is that the slip-predictable model provides neither a precise nor an accurate estimate of the time of the next Parkfield earthquake.

The geodetic data set for Parkfield is the best in the world, and it has permitted a very detailed slip-budget balance to be carried out for two separate time periods. *Segall and Harris* [1987] and *Harris and Segall* [1987] used trilateration data collected between 1960 and 1984 to estimate the spatial variation of fault slip with depth as well as along strike for the 1966 Parkfield earthquake and for the beginning of the current interseismic period. These studies estimated a range of strain reaccumulation times of 14-25 years, with even the most extreme choices of adjustable parameters yielding strain-reaccumulation times no longer than 29 years. Recently, *Murray et al.* [2001] used data from 15 GPS campaigns to show that the distribution of interseismic slip over the fault plane was unchanged, to within the resolution of these data. Both studies imply that enough strain energy to produce another 1966-size Parkfield earthquake had reaccumulated no later than 1995, and probably as much as ten years earlier. Although a ten-year error in the time of the earthquake may seem small, ten years is at least one-third of Parkfield's average recurrence interval. Proportional errors for more infrequent earthquakes could easily exceed the 30-year time frame popular for seismic probability forecasts.

The non-occurrence of the Parkfield earthquake despite the reaccumulation of sufficient strain implies that either the slip-predictable earthquake recurrence model is not valid, or that the next $M6$ earthquake will be larger than the 1966 event. Cruder strain budget balanced are a mainstay of earthquake probability forecasts, but there is no reason to suppose they foretell recurrence intervals more accurately than at Parkfield.

When the Parkfield fault segment next ruptures, will the earthquake involve more slip than previous Parkfield earthquakes? Will it release only part of the strain energy? The answers to these questions can plainly help guide improvements to the slip-predictable model that will pay off in more accurate probability calculations.

Map of Aseismic Slip Distribution at Depth along the Fault

Geodetic measurements and seismic monitoring have allowed the distribution of aseismic slip rate over the fault plane to be mapped, and in some cases, its variation with time to be detected. Mapping of the time history of propagating seismic ruptures is becoming routine, but Parkfield is the first location where aseismic slip can be mapped with useful precision. Moreover, microearthquake observations and geodetic measurements yield two independent estimates of this slip distribution.

Geodetic data are usually sufficient only to estimate the slip rate of a single rectangular section of fault plane many kilometers on a side. Current implementations of the slip-predictable recurrence model (e.g., WG99) employ an "aseismic slip factor", to account for the unknown spatial distribution of interseismic slip over the anticipated rupture plane. The excellent spatial coverage of geodetic measurements at Parkfield, however, allows subdivision of the fault into 2x2-km areas with an estimate of slip rate in each area. The resolution of the data has been adequate to resolve spatial variations in slip rate beginning in the interseismic period prior to the 1966 event. The *Harris and Segall* [1987] interseismic slip distribution inferred from the geodetic measurements clearly defines the locked section of the fault where no background microseismicity is occurring.

The coincidence of the locked patch, as determined geodetically, with the fault area having low background seismicity, supports the idea that portions of the fault with low microseismicity are in fact slipping at a rate less than the nominal plate-rate of $33mm/yr$. The detailed mapping of the spatial slip variations also allows the slip budget balance to be made more carefully for Parkfield than at other locations.

Repeating Earthquakes and Foreshocks at Parkfield

The Parkfield fault segment is seismically active with about 2 events $M \geq 2$ in a typical month. The intensification of the USGS's Northern California Seismic Network (NCSN) in the Parkfield segment and the UC Berkeley High Resolution Seismic Network (HRSN) allow microseismicity to be detected reliably at magnitude < 1 and located to within $\pm$ 200 m vertically as well as horizontally. Much more refined locations are possible with special techniques. *Cole and Ellsworth* [1995] have shown that families of repeating earthquakes account for many of the $M \geq 4$ earthquakes near Parkfield, with discrete fault patches apparently capable of generating identical earthquakes both before and after the 1966 Parkfield earthquake. Recent work by *Nadeau and McEvilly* [1999] on repeating microearthquakes recorded by the borehole HRSN and surface seismometers (NCSN) indicates that these small, precisely located events repeat at intervals dependent on fault slip rate (Figure 3). They exploited this observation to show that in 1992-1993, the slip rate increased over a portion of the fault at depth beneath Middle Mountain. The underlying physical mechanism of the repeating earthquakes is unknown, but is consistent with the idea that individual strong patches of fault repeatedly fail as units in response to tectonic loading.

Study of background seismicity at Parkfield has great potential to advance our understanding of foreshocks. Foreshocks precede 10% to 50% of earthquakes, so techniques for discriminating between foreshocks and background seismicity would constitute major progress toward the capability to issue meaningful earthquake warnings. At this time, however, the physical processes linking foreshocks and mainshocks are not understood, and no consistent features of foreshocks have been identified based on study of seismograms alone.

In both 1934 and 1966, $M5$ foreshocks preceded Parkfield mainshocks by 17 minutes, and these two foreshocks were representatives of the same repeating earthquake family. In 1992-1994, three earthquakes with $M > 4$ occurred closer than three km to the southeast of

the 1966 hypocenter, and all ruptured toward that point, but none was either a foreshock or grew into a $M6$ mainshock. Coseismic rupture mapping by modeling waveforms of these earthquakes at Parkfield has been completed by *Fletcher and Spudich* [1998] and *Fletcher and Guatteri* [1999], and the resulting slip distributions can be used to show that in particular, the December 20, 1994, $M5$ earthquake increased the shear stress favoring failure at the 1966 hypocenter by more than 1 bar. The three earthquakes also occurred at a time when the slip rate over part of the fault was increasing, as described below. However, none of these three earthquakes belonged to the same family as the 1934 and 1966 17-minute foreshocks. Questions raised by these earthquakes include whether a future Parkfield earthquake will have a foreshock rupturing the same area as the 1934 and 1966 17-minute foreshocks, and whether such foreshocks, should they occur, will be followed by non-steady-state aseismic deformation leading to the mainshock.

It is also important that the largest foreshocks of the great, $M > 8$, 1857 Fort Tejon earthquake occurred near Parkfield one and two hours beforehand. [*Meltzner and Wald*, 1999]. Although a full repeat of the Fort Tejon earthquake is not expected at this time, the postseismic behavior of the southern end of the Parkfield segment will be of great interest for assessing stress transfer to the locked section of the San Andreas fault farther southeast.

Detecting Departures from Steady-State Strain Accumulation

Current practice for estimating earthquake recurrence intervals uses contemporary strain rates measured across earthquake source zones, assumed to be time-invariant throughout the interseismic strain accumulation period. At Parkfield, however, geodetic data are precise enough, and the record is long enough, to document time variations in the rate of strain accumulation. The hope is that these time variations contain information that can be used to estimate the time of the next $M6$ earthquake with higher accuracy than a strain-budget balance that assumes a time-invariant strain rate.

1. 1966 Postseismic Slip

Postseismic slip was first documented by *Smith and Wyss* [1968] for the 1966 Parkfield earthquake using repeated surveys across the fresh surface rupture in the days following the earthquake. The creepmeter CRR1 (Figure 4), installed at one of their sites, continues this record to the present, and is still operating. In the first months following the 1966 earthquake, 120 mm of postseismic slip occurred, followed by a period of 11 years, ending in 1977, in which slip occurred at a relatively constant rate of 11 mm/year. In 1977, creep rate decreased at CRR1. Transitions between these rates appear abrupt, rather than gradual. These changes in strain rate are barely discernible in the trilateration data utilized by *Segall and Harris* [1987] and *Harris and Segall* [1987], which were measured at intervals of years to months, and for which typical error bars are 20 mm. No other instruments at Parkfield were operating at this time.

2. Steady-state Interseismic Period

The records from many of the creepmeters show both a relatively stable background slip rate punctuated by rapid slip or "creep" events lasting a few hours or days. These creep events are often accompanied by strain and water-level changes, which taken together imply that slip during these events extends to depths of only a few hundred meters. Trilateration, and more recent EDM and GPS observations, do not resolve these time variations because of their measurement errors are too large and the creep events are too shallow.

3. Remotely Triggered Strain-Rate Changes

The $M6.7$ Coalinga earthquake in 1983 perturbed the rate of fault creep at Parkfield. It has been suggested by *Simpson et al.* [1988] and more recently by *Toda and Stein* [2001] that the static stress changes from the Coalinga earthquake changed the normal stress on the San Andreas fault. *Toda and Stein* [2001] argue that this stress change effectively clamped the San Andreas at Parkfield and has delayed the recurrence of the characteristic Parkfield earthquake.

4. 1992-2001 and beyond

In late 1992, microearthquake activity increased, rates of lengthening accelerated on several two-color EDM lines, and shear-strain rates measured by two borehole strainmeters increased (Figure 5) [*Gwyther et al.*, 1997;*Langbein et al.*, 1999; *Gao et al.*, 2000]. The deformation data are consistent with a period of faster fault slip beneath Middle Mountain as inferred from decreasing recurrence intervals of repeating microearthquakes. Several creepmeters recorded increased creep rates, including the CRR1 creepmeter, which is relatively free of the effects of rainfall. The BTSM data and the two-color EDM lines indicate deceleration in 1997-1998, although at the end of 2000, several of these instruments still indicated higher slip rates than their 1988-1992 averages. Creep rate at CRR1 has remained at the elevated rate reached in 1993. The rate change on all instruments resembles a fairly abrupt shift during a 3-year period when the four largest earthquakes near the 1966 hypocenter occurred since the start of geodetic monitoring.

To date, there have been few recordings of strain rate variations on any plate boundary, and Parkfield data are unique because four types of independent measurements simultaneously indicate these changes. In addition, a rigourous noise analysis has been applied to the strain and EDM data to verify the statistical significance of these changes.

This observation begins to answer three key questions about interseismic fault slip: (1) how do interseismic strain accumulation rates vary with time, how much of this variation is random, and how much reflects the evolution of the fault state as the earthquake cycle progresses? (2) how do strain changes measured near the ground surface relate to processes on the deeper parts of the fault where earthquakes initiate? and (3) at what magnitude can displacement or strain changes be detected within the noise of each instrument? These issues are important to using contemporary geodetic observations to estimate earthquake recurrence times, and have been identified as primary scientific goals of the Plate Boundary Observatory.

5. Premonitory

One unanticipated benefit of the Parkfield monitoring was the observation of water-level and strain changes beginning three days prior to the 1985 $M5$ Kettleman Hills earthquake, which occurred 35 km northeast of Parkfield. These changes may have been caused by aseismic slip preceding the Kettleman Hills event but this inference is difficult to establish because there were no other deformation monitoring instruments near this earthquake.

Anomalous electromagnetic changes were detected prior to a $M5$ earthquake in 1994 [*Fraser-Smith and Liu*, 1995]. This ULF instrument was located approximately 10 km from the earthquake.

Properties of Fault and Nearby Crust

Detailed geophysical studies of the San Andreas fault at Parkfield have two goals. One is to characterize the structure and composition of the fault zone in enough detail to discriminate among competing theories of earthquake generation, including theories based on the presence of pore fluids. The other goal is to seek correlation of fault zone geophysical signatures with the spatial and temporal distribution of seismicity, mainshock slip, and interseismic slip.

Both goals have important implications for earthquake hazard assessment in other areas. First, if fluid-pressure based theories of fault failure are applicable, then earthquake recurrence intervals based on conservation of strain energy will require substantial modification. Second, if geophysical properties can delineate earthquake rupture zones at Parkfield, then the same properties could also be used to identify fault segments in other locations.

Earthquake probability forecasts require the identification of endpoints of seismogenic fault segments, commonly placed at geometric irregularities of surface fault traces. Parkfield provides a test of this methodology. The surface trace of the fault makes a 5° bend just north of the 1966 epicenter and steps 1 km SW near Gold Hill. These two points have been used to define the Parkfield segment, because the 1966 $M6$ earthquake nucleated near the 5° bend and the rupture front decelerated at Gold Hill. For these features to initiate and arrest seismic rupture, however, they must extend to depths of several km. or more. Yet when Parkfield background seismicity is relocated with a 3-D velocity model, hypocenters do not show the 5° bend or the fault trace step at Gold Hill [*Nishioka and Michael*, 1990; *Aviles and Michael*, 1990; *Eberhart-Phillips and Michael*, 1993].

Several studies of seismic wave velocities around Parkfield have identified bodies at seismogenic depths with velocities or attenuation that could be caused by high fluid pressure. Between depths of 6 and 10 km, there is a 3-km-wide zone of low V_p [*Eberhart-Phillips*, 1993], relatively lower V_s, and therefore high V_p/V_s [*Michelini*, 1991] immediately northeast of the active fault surface as defined by microseismicity. Along strike of the San Andreas fault, this body extends from the 1966 hypocenter about 5 km to the southeast [*Michelini*, 1991; *Johnson*, 1995]. This zone also has high attenuation. The seismic wave propagation characteristics of this body are consistent with high fluid content, but do not require pressure in the fluid to be elevated above hydrostatic. High fluid pressure in a 1 km-deep borehole on the northeast side of the fault in this area, however, shows that there is at least localized overpressure at depth.

Unsworth et al. [1997] conducted a magnetotelluric transect across the fault on Middle Mountain, directly above the northeastern limit of the high V_p/V_s body. The prominent finding is a vertical zone of low resistivity along the fault trace, about 500 m wide, extending to about 4 km depth, with higher resistivities, or narrower width, at greater depth. This zone contains areas of resistivity which is too low to be explained by the presence of clays or serpentinite, and therefore strongly indicates a network of interconnected, fluid-filled pore space. *Li et al.* [1990] previously inferred the existence of a seismic low-velocity zone of similar width to model seismic trapped waves in the fault zone. The seismic low velocity zone would require at least some of the fault-zone fluid to be distributed in pores, rather than localized in cracks.

The previous studies show that bodies that might contain fluids are likely present. *Johnson and McEvilly* [1995]'s analysis of HRSN waveform data suggests that many of the small, repeating earthquakes might represent hydrofracture of high-fluid-pressure pockets rather than being shear displacement on the fault.

Full-cycle Earthquake Models

It has been possible to construct fault models that numerically simulate fault slip, fault stress, and crustal deformation for an entire $M6$ earthquake cycle at Parkfield. In these models, the fault is idealized as a vertical plane in a uniform elastic half space. The resistance of the fault plane to sliding is assumed to be governed by a rate- and state-dependent friction law, which is an excellent model for rock friction in the laboratory and contains sufficient complexity to yield aseismic slip, seismic rupture, and aftershocks. A spatial distribution of frictional properties over the fault plane is assigned, broadly consistent with the observed spatial distribution of slipping and locked patches. In response to uniformly increasing shear stress imposed by plate motions, the model computes fault slip and stress as functions of time and position on the fault plane. The overall simulated fault slip rate naturally exhibits coseismic, postseismic, interseismic, and preseismic stages of an earthquake cycle. On some patches of the fault, progressive aseismic slip leads to decreased frictional resistance, with the potential for the slip rate to increase many orders of magnitude in an unstable manner. Such an instability constitutes a simulated earthquake. Generally speaking, computed postseismic and preseismic stages each take a small fraction of the earthquake cycle and are times of decreasing and increasing fault slip rate, respectively. The interseismic stage takes most of the earthquake cycle time and has relatively constant (but spatially variable) slip rate.

One virtue of these models is that they are well-posed boundary value problems in which parameter values of an assumed fault friction law completely determine the time of the instability and the crustal deformation history. In particular, the fault slip instability that is an earthquake analog is a computed result that depends in part on the rate of fault weakening at the end of the earthquake cycle. Adjusting the parameters in these instability models to agree with geodetic data provides constraints on the physical properties of the fault.

Simulations with the model of *Stuart et al.* [1995a], *Stuart et al.* [1995b], and *Tullis* [1996], when modified to have two strong fault patches instead of one for the $M6$ slip, agree reasonably well with most fault creep records, including the portions associated with the 1992 anomaly mentioned above. Because theoretical creep and strain rate minima occur about halfway through an earthquake cycle, and the actual CRR1 minimum creep rate was around 1983, the simulation has the interesting interpretation that the present Parkfield cycle is near its end. In this view, the observed increased seismicity and deformation rates are just an irregular instance of predicted slip rate increase late in an earthquake cycle. The model has a smooth spatial variation of fault strength, and rates would be less regular with more complicated variation of fault strength. *Stuart et al.* [1995a] and *Tullis* [1996] found for some cases that theoretical nonlinear changes in borehole strain would be large enough to detect several months before a $M6$ earthquake.

Full-cycle fault models have a direct application to the prediction component of earthquake hazard estimation. Since an earthquake in a model is part of the mathematical solution to the associated differential equations (unlike, say, the unphysical failure conditions of a preset slip deficit, failure stress, or Coulomb condition), the time of the earthquake is predictable from the prior faulting history. An accurate model consistent with past instrumental observations can extrapolate faulting a short time into the future to estimate future actual faulting. Geodetic data can in principle be inverted for fault friction parameters, yielding a calibrated model that can compute predicted times of earthquakes. Such models constitute a framework for unified treatment of physical theory, observational data and prediction of future faulting at Parkfield.

The prototype full-cycle fault model for Parkfield is roughly consistent with some geodetic data, and the model predicts increasing deformation rate near the end of an earthquake cycle. The model needs more details of fault property variation, and a set of simulations should be run to find best agreement with all deformation data and to estimate the uncertainty of the time of the next $M6$. We suspect that the calculated uncertainty of a future earthquake will be large unless strong nonlinear preseismic deformation somehow places a tight constraint on model parameters. But at least the above procedure allows analysis to determine the mathematical or physical reasons. That is, there is way to understand why prediction of earthquake times and ground shaking is difficult and to discover circumstances when it might be easier.

It would also be useful to construct new full-cycle models that contain other physical ideas such as pore fluid effects or irregular fault geometry. All full-cycle models should be generalized to calculate seismic ground motion from model parameter values estimated from pre-earthquake deformation data.

Instrument Research and Development

At Parkfield, data from a variety of instruments can be compared to help identify geophysically significant signals. However, each instrument has limits to its spatial and temporal resolution. These limits have been rigorously characterized for several types of instruments. For instance, *Langbein et al.* [1993] examined creep, water-level changes,

and EDM to quantify the temporal sensitivity of each technique, and *Park and Fitterman* [1990] determined the sensitivity limits of their telluric experiment. Several problems that limit sensitivity have been identified, and other techniques that attenuate noise have been demonstrated. Below is a short list of problems and solutions.

1. High precision (EDM) measurements at Parkfield revealed that the long-term precision of geodetic time series can be seriously degraded by localized monument motion. Deeply braced monuments with better stability have been shown to improve the precision of geodetic measurements and such monuments are now being used for continuous GPS stations in southern California.

2. Surface measurements of fault creep contain information about the shallow slip rate on the San Andreas fault, but many such instruments are affected by rainfall. Fortunately, the CRR1 creepmeter at Parkfield, at a site where fault slip has been measured since shortly after the 1966 Parkfield earthquake, is relatively free of the effects of rainfall, and has accumulated a data set documenting accelerated post-seismic creep, a fairly steady interseismic rate, and accelerated creep beginning in early 1993.

3. Borehole strainmeter records at Parkfield have shown that shear strain components recorded by three-component borehole strainmeters are less affected by subsurface fluid pressure variations than volumetric strain, and can accurately track strain rate changes that take place over periods of months to years. Both three-component and volumetric borehole strainmeters have recorded strain changes lasting hours to days, with amplitudes of order 10^{-8}, that correlate with surface fault creep.

4. Water-level monitoring at Parkfield has yielded a possible example of a fluid-pressure precursor to the 1985 Kettleman Hills, California, earthquake (35 km NE of Parkfield) [*Roeloffs and Quilty*, 1997] and many examples of water-level changes induced by fault creep [*Roeloffs et al.*, 1989]. Step-like water level changes associated with a $M5$ earthquake near Parkfield in 1994 showed that at 4 of 8 sites, coseismic fluid pressure changes closely match those that would be expected from simple models of the volumetric strain distribution following an earthquake [*Quilty and Roeloffs*, 1997]. On the other hand, one monitored well exhibits water-level rises in response to both distant and local earthquakes, and is an example of a site where fluid-pressure changes of tectonic origin cannot be explained by existing models of elastic-pressure coupling [*Roeloffs*,1998].

5. Installing seismometers in boreholes, instead of at the ground surface, greatly improves their sensitivity to micro-earthquakes. Waveforms from the borehole network have better fidelity because they are not contaminated by surface noise and this improved sensitivity allows more earthquakes to be detected and studied. The data from the Parkfield downhole HRSN have been used in conjunction with the NCSN surface instruments to examine several items including temporal changes in travel-time, trapped waves in the fault zone, the location, size, and times of repeating earthquakes.

Recommended Instrument Upgrades

Currently, most of the fieldwork by the USGS and other institutions is simply to maintain instruments, many of which use obsolete technology. Moreover, many of the instrument locations were guided by the forecast that a moderate earthquake would occur within a decade of installation. The accumulated data sets have revealed that some sites and instruments provide much more useful data than others.

The following recommendations for each kind of instrument are based on these criteria:

• Decommission poorly functioning instruments or those whose benefit does not justify their cost.

• Replace critical instruments with modern installations that will provide better data and require less maintenance. Critical instruments are those for which there is already a high-quality data set, and which help constrain the spatial and temporal distribution of fault slip rate.

• Increase coverage in the anticipated nucleation zone of the next $M6$ event near Middle Mountain.

• Increase coverage to give maximum resolution of fault properties for fault models over the entire $M6$ rupture area.

Creepmeters

Continuation of fault creep measurement is important for two reasons: (1) many of the signals seen on borehole strainmeters are due to surface fault slip, and (2) most fault models of inter-seismic slip at depth depend upon measurement of surface slip. However, many of the current creepmeters are at the ends of their useful lifetimes because the Invar wires used to measure distance between monument pairs are rubbing against their buried culverts. In addition, many creepmeters are noisy due to rainfall-induced and random-walk motions of their monuments. We now know how to improve creepmeter performance by using deeply braced (10 m deep) monuments similar to those used for continuous GPS stations.

Of the current twelve creepmeters (Figure 1), we should retain and upgrade seven: xsc1, xmm1, xva1, xta1, wkr1, crr1, xgh1. All need new monuments. Other types of displacement transducers should be evaluated to determine if maintenance requirements can be reduced. The remaining creepmeters should either be decommissioned or allowed to run until they fail. Estimated cost would be about \$30K/site for each of seven creepmeters, or a total of \$210K.

GPS

By early 2001, GPS stations will be located at 7 of the 18 two-color EDM sites. It is anticipated that the EDM measurements will be terminated shortly since it is difficult to maintain an instrument using 25 year-old technology, and because the operator, Duane Hamann, has retired and moved from Parkfield. With the lack of personnel, EDM measurements are currently made once every three weeks by project personnel driving from either Menlo Park or Mammoth Lakes, CA. If we want to continue the baseline data from

this network, which was started in the mid-1980s, we need to install additional GPS receivers at two-color EDM sites. In fact, the current distribution of co-located GPS and EDM sites does not include the three baselines that provided the best detection of the 1993 strain anomaly. Also, the current distribution of GPS sites tends to favor the northwestern part of the network near Middle Mountain.

We recommend installation of GPS receivers at the following six EDM sites, listed from highest to lowest priority: Hunt or Turk, Buck, Mason, Gold, Creek, Nore. These stations include the sites of the 1993 anomaly (Hunt or Turk, and Buck), provide information on slip and strain in the southeastern part of the network (Mason, Gold, and Creek), and provide near-surface slip information for the central site at Carr (Nore). The estimated cost of these GPS receivers is about $30K/site for a total of $180K

Dilatometer and Tensor Borehole Strain

The measurements in SAFOD of fault-zone properties, fluid pressure, and strain at 4 km below the surface will be most valuable if supplemented by three additional 3-component strainmeters nearer the surface at distances of 1 to 5 km from the deep borehole. Because SAFOD only provides a measurement of slip at a single location, the additional strain measurements would be needed to constrain the dimensions of a slipping fault area detected in the deep borehole. Currently, there is an opportunity to install strainmeters in two holes that will be drilled in Spring, 2001, as part of an NSF-funded upgrade of the HRSN in support of SAFOD.

The dilatometers and borehole tensor strainmeters are the primary instruments that can detect aseismic processes linking immediate foreshocks to the mainshock, or a Parkfield rupture to aseismic deformation of the currently locked Cholame segment to the southeast. However, it is difficult to interpret strainmeter data accurately in the immediate aftermath of a nearby earthquake because strain associated with seismic waves over-ranges these instruments. Future strainmeters at Parkfield should be designed to overcome this limitation, if at all possible. Also, the data pathway for high-frequency recording of strainmeter data needs to be revitalized so that adequate sampling is obtained if the foreshock-mainshock interval is similar to those in 1934 and 1966 (17 minutes). The strainmeters are capable of providing meaningful data when sampled once per second, but current installations record samples only every ten minutes.

Originally, there were eight dilatometers installed at Parkfield. Currently, five of these instruments are still working, although one of these may be starting to fail. We recommend that all five be continued, with especially high priority for the Frohlich and Donalee sites, which have provided the highest-quality data. We also recommend that all three tensor strainmeters (Eades, Frohlich, and Donalee) be continued, and that two new tensor strainmeters be installed in SAFOD holes. A third new instrument should be installed at Gold Hill to replace failed dilatometers there; this site is key to understanding stress transfer to the Cholame segment. The estimated cost to install tensor strainmeters is about $50K/site including drilling. Savings of $20K to $30K/site is possible if we take advantage of the boreholes for the HRSN upgrade.

Water-Level Monitoring

Several water-level monitoring stations have been discontinued; the remaining seven are BV, MM, JC, FF, TF, GH, and HR (Figure 1). Pore fluid pressure is also monitored in the Varian deep borehole, but the data do not appear to be of high quality, and the installation is too deep to repair. All of the shallower holes have shown water-level changes of tectonic origin, and should be continued, with perhaps lower priority for TF and FF. Recently it has been recognized that borehole strain data can be more confidently interpreted if there is a record of formation fluid pressure from a co-located site. Therefore, fluid pressure sensors should be installed in the boreholes with new 3-component strainmeters, pending evaluation of data from similar installations in other countries. If such installations are satisfactory, the the $50K cost per 3-component strainmeter site includes the installation of a pressure sensor in the same borehole. If an additional borehole would need to be drilled, then there would be an additional drilling cost of $20-$30K/site.

Magnetometer

The total-field magnetometers operated by the USGS at seven sites near Parkfield should be evaluated to determine if they provide useful information beyond that obtained from electromagnetic monitoring by university researchers.

Northern California Seismic Network (NCSN)

Because the current microwave telemetry link between Parkfield and Menlo Park is becoming obsolete, NCSN will be changing to satellite communication. The new system will be digital with improved dynamic range. However, the weak link will be the FM telemetry used to move the analog data from each seismometer to the satellite up-link. If ANSS is approved then each seismic station will be digital. We should take advantage of ANSS to install FBA (Force-balanced accelerometers) sensors (broadband, 3 component, and large dynamic range) at a few NCSN sites. These instruments will improve the strong motion network and provide some strong motion data in real-time.

UC Berkeley High Resolution Seismic Network (HRSN)

After several years of decay due to obsolete equipment, this network is currently being upgrading with both USGS external funding and NSF funding in support of siting for SAFOD. Three stations are being added north of the current network to improve location of small earthquakes in the immediate neighborhood of the proposed SAFOD. In addition, the network has completely replaced its telemetry with reliable modern equipment. As mentioned above, boreholes for the new instruments should include strainmeters. Currently, pore-pressure sensors, televiewer logging, electrical dipole monitoring, and heat flow measurements will be conducted in these holes. Unfortunately, no strainmeters are immediately available for installation. If strainmeters become available, we could install them into two of the holes in Spring 2001 when they are drilled.

The research results from the HRSN have been impressive. We recommend that this network be continued since the data from this network has contributed greatly to extending cutting-edge seismological research.

California Strong Motion Instrumentation Program Array (CSMIP)

This project, run by the State of California, is slowly upgrading its instruments throughout the state, but Parkfield does not appear to be a high priority. The State has removed the original Electric Power Research Institute (EPRI) dense array of strong-motion instruments. It would appear that we could assist by complementing this network of triggered FBAs with our own set of FBA's as part of the NCSN upgrade.

USGS Parkfield Small Aperture Array (UPSAR)

Many of the original goals for this network have been achieved. The exception obviously is recording of a $M6$ Parkfield earthquake. Data from UPSAR will provide information on the directivity of seismic waves which will allow detailed study of the seismic rupture. Other arrays of FBAs could be operated in the area to complement the UPSAR data. Currently, the 14 UPSAR sensors are linked together as part of local area network and data are telemetered to Menlo Park. Maintenance and repair of the current system costs about \$10k/year. Switching to triggered on-site recording might reduce this cost, but would require an investment of \$100K. Because dense arrays capture the directivity of seismic waves better than distributed instruments, a second array similar to UPSAR should be considered, possibly at the site of the old EPRI array. The cost for the second array would be about \$100K.

General Earthquake Observation System (GEOS)

Given the distribution of other FBA instruments near Parkfield, the few GEOS instruments are not worth keeping because they are linked to the old-technology GEOS data logger which require several site visits during the year. We recommend that these sites be decommissioned.

Telemetry

With the rapidly changing technology, the current means that we retrieve data from the field electronicly is becoming obsolete. The current seismic telemetry, as discussed above, is obsolete because it relies on a microwave link for which components are not longer being made. We expect that it will be replaced with a satalite based system. In addition, many of the monitoring experiments needing low-bandwidth telemetry are being faced with the prospect that the current system will become obsolete. These monitoring experiments include the strainmeter, creepmeter, and water well networks. The current system will need to replaced with more modern equipment. And, in the case of the strainmeters, there is a need for some higher bandwidth telemetry to replace the GEOS system so that we can capture the details of any pre-seismic events should they occur. Recall that we recommend that the GEOS be decommissioned.

The GPS data also require telemetry. The current set-up uses radio modems to move the data from the remote receivers to a central site at Parkfield. The data are then moved from the computer at the central site to USGS's Pasadena office over the telephone. Although the phone charges are paid for by office overhead, it might be cheaper in the long-run to use satalite telemetry. In addition, the radio-modem network might be overloaded when

other experiments come on-line. This might be the case this summer when the seismic network installed by U. Wisconsin and RPI becomes operational.

The above illustrates the need to examine our telemetry requirements carefully so that, if possible, financial resources can be pooled together to buy and maintain a telemetry system useful for more than one project, and that the telemetry from one network does not interfer with another.

Personnel Requirements

To gain the fullest benefits from the Parkfield experiment, we need at least two people to fulfill certain tasks. One individual is needed to maintain the instruments in the field. A second person is needed to conduct research into fault modeling.

We have had at least one technician stationed at Parkfield since 1986. The incumbent technician is requesting a disability retirement. Given the hiring ceilings and budget limits, this job could easily be administratively eliminated. The assumption by administrators is that a few individuals from the Menlo Park staff could do the maintenance. However, the Menlo Park technical field staff is already fully committed since they also have responsibility to maintain increasing numbers of instruments elsewhere in California. We believe that the Parkfield experiment requires that a new technician be hired to replace the current technician.

In writing this report, it became apparent that a number of numerical fault simulations should be calculated to better understand the possible relation between fault zone properties, the deformation data, and earthquake locations. We have fault modeling expertise in house, but the individuals are committed to other projects. We believe that much of the analysis could be accomplished by either a post-doctoral fellow or through a contract to a research group with expertise in fault modeling.

References

Bakun, W.H., and Lindh, A.G., The Parkfield, California, earthquake prediction, Science 229. 619-624, 1985.

Bakun, W.H., and McEvilly, T.X., Parkfield ... , Jour. Geophys. Res. 00, 00-00, 1985.

Gao, S., P.G. Silver, and A.T. Linde, Analysis of deformation data at Parkfield, California: Detection of a long-term strain transient, J. Geophys. Res., 105 (B2), 2955-2967, 2000.

Gwyther, R.L., M.T. Gladwin, M. Mee, and R.H.G. Hart, Anomalous tensor strain at Parkfield during 1993-1994, Geophys. Res. Lett., 23, 2425- 2428, 1996.

Langbein, J., R. Gwyther, R. Hart, and M.T. Gladwin, Slip rate increase at Parkfield in 1993 detected by high-precision EDM and borehole tensor strainmeters, Geophys. Res. Lett., 26, 2529 2532, 1999.

Meltzner, A.J., and Wald, D.J., Bull. Seismol. Soc. Am. 89, 1109-1120, 1999.

Michael, A.J., and Jones, L.M., Bull. Seismol. Soc. Am. 88, 117-130, 1998.

National Earthquake Prediction Evaluation Working Group, Earthquake Research at Parkfield, California, for 1993 and beyond, U.S. Geological Survey Circular 1116, 14pp., 1994.

Parkfield Working Group, Bakun, W.H., and 14 others, Parkfield, California, earthquake prediction scenarios and response plans, U.S. Geological Survey Open-File Report, 87-192, 50pp, 1987.

PBO Steering committee, The Plate Boundary Observatory; Creating a four-dimensional image of the deformation of Western North America, http://www.unavco.ucar.edu/community/publications/proposals/PBOwhitepaper.pdf, 2000.

Roeloffs, E., The Parkfield, California, Earthquake Experiment: An update in 2000., journal, 00, 000-000, 19xx.

Roeloffs, E. and Langbein, J., The earthquake prediction experiment at Parkfield, California, Reviews of Geophysics 35, 315-336, 1994.

Stuart, W.D., and T.E. Tullis (1995). Fault model for preseismic deformation at Parkfield, California, *J. Geophys. Res.* 100, 24,079–24,099.

Zoback, M.D., Hickman, S.H., and Ellsworth, W.L., Scientific Drilling into the San Andreas Fault at Parkfield, CA: Project overview and operation; Proposal prepared for the National Science Foundation, http://pangea.Stanford.EDU/∼zoback/FZD/, 1998.

Parkfield Bibliography

Allen, C.R., and S.W. Smith, Parkfield earthquake of June 27-29, 1966, Pre-earthquake and post-earthquake surficial displacement, Bull. Seismol. Soc. Am., 56, 955-967, 1966.

Archuleta, R.J., and S.M. Day, Dynamic rupture in a layered medium: The 1966 Parkfield earthquake, Bull. Seismol. Soc. Am., 70 (3), 671-689, 1980.

Armstrong, B.H., C.M. Valdes, Acoustic emission/microseismic activity at very low strain levels in Acoustic Emission: Current Practice and Future Directions, edited by W. Sachse, J. Roget, and K. Yamaguichi, ATSM Spec. Tech. Publ., STP 1077, 358-364, 1991.

Bakun, W.H., J.D. Bredehoeft, R.O. Burford, W.L. Ellsworth, M.J.S. Johnston, L. Jones, A.G. Lindh, C.E. Mortensen, E. Roeloffs, S. Schulz, P. Segall, and W. Thatcher, Parkfield earthquake prediction scenarios and response plans, U.S. Geological Survey Open-file Report, 86 365, 1986.

Bakun, W.H., and A.G. Lindh, The Parkfield, California earthquake prediction experiment, Science, 229, 619-624, 1985.

Bakun, W.H., and T.V. McEvilly, Are foreshocks distinctive? Evidence from the 1966 Parkfield and the 1975 Oroville, California sequences, Bull. Seismol. Soc. Am., 69, 1027-1038, 1979a.

Bakun, W.H., and T.V. McEvilly, Earthquakes near Parkfield, California: Comparing the 1934 and 1966 sequences, Science, 205, 1375-1377, 1979b.

Bakun, W.H., and T.V. McEvilly, P-Wave spectra for ML 5 foreshocks, aftershocks, and isolated earthquakes near Parkfield, California, Bull. Seismol. Soc. Am., 71 (2), 423-436, 1981.

Bakun, W.H., and 14 others (a.k.a, The Parkfield Working Group), Parkfield, California, earthquake prediction scenarios and response plans, U.S. Geological Survey Open-File Report, 87-192, 50pp, 1987.

Ben-Zion, Y., and P. Malin, San Andreas fault zone head waves near Parkfield, California, Science, 251. 1592-1594, 1991.

Ben-Zion, Y., J.R. Rice, and R. Dmowska, Interaction of the San Andreas fault creeping segment with adjacent great rupture zones and earthquake recurrence at Parkfield, J. Geophys. Res., 98 (B2), 2135-2144, 1993.

Bernardi, A., A.C. Fraser-Smith, P.R. McGill, and O.G. Villard Jr., ULF magnet field measurements near the epicenter of the M7.1 Loma Prieta earthquake, Phys. Earth Planet. Inter., 68,45-63, 1991.

Borcherdt, R.D. and 8 others, A general earthquake observation system (GEOS), Bull. Seismol. Soc. Am., 75, 1783-1825, 1985.

Brown, R.D.J., J.G. Vedder, R.E. Wallace, E.F. Roth, R.F. Yerkes, R.O. Castle, A.O. Waananen, R.W. Page, and J.P. Eaton, The Parkfield-Cholame, California, earthquakes of June August 1966, U.S. Geological Survey, Menlo Park, CA., 1967.

Daley, T.M., and T.V. McEvilly, Shear-wave anisotropy in the Parkfield Varian well VSP, Bull. Seismol. Soc. Am., 80 (4), 857-869, 1990.

Davis, P.M., D.D. Jackson, and Y.Y. Kagan, The longer is has been since the last earthquake, the longer the expected time till the next?, Bull. Seismol. Soc. Am., 79, 1439-1456, 1989.

Eaton, J.P., M.E. O'Neill, and J.N. Murdock, Aftershocks of the 1966 Parkfield-Cholame, California, earthquake: A detailed study, Bull. Seismol. Soc. Am., 60 (4), 1151-1197, 1970.

Eberhart-Phillips, D., and A. Michael, Three-dimensional velocity structure, seismicity, and fault structure in the Parkfield region, central California, J. Geophys. Res., 98, 15,737-15,758, 1993.

Fitzpatrick, C., and P.W. O'Brien, Social response to the first "A" alert of the Parkfield Earthquake Prediction Experiment, Natural Hazards Research and Applications Information Center, 1-22, 1992.

Fletcher, J.B., L.M. Baker, P. Spudich, P. Goldstein, J.D. Sims, and M. Hellweg, The USGS Parkfield, California, Dense Seismograph Array: UPSAR, Bull. Seismol. Soc. Am., 82, 1041 1070, 1992.

Fletcher, J.B., and M. Guatteri, Stress Drop for three M 4.3-4.7 (1992-1994) Parkfield, CA, earthquakes, Geophys. Res. Lett., 26 (15), 2295-2298, 1999.

Fletcher, J.B., and P. Spudich, Rupture characteristics of the three M 4.7 (1992-1994) Parkfield earthquakes, J. Geophys. Res., 103, 835-854, 1998.

Fletcher, J.B., L.M. Baker, P. Spudich, P. Goldstein, J.D. Sims, and M. Hellweg, The USGS Parkfield, California, dense seismography array: UPSAR, Bull. Seismol. Soc. Am., 82, 1041-1070, 1992.

Fraser-Smith, A.C., and T.T. Liu, ULF magnetic field variations preceding the M 5.0 earthquake of 20 December 1994 at Parkfield, California, Supplement to EOS, Trans. Am. Geophys. Union, 76 (46), F360, 1995.

Gao, S., P.G. Silver, and A.T. Linde, Analysis of deformation data at Parkfield, California: Detection of a long-term strain transient, J. Geophys. Res., 105 (B2), 2955-2967, 2000.

Gladwin, M.T., R.L. Gwyther, R. Hart, M.F. Francis, and M.J.S. Johnston, Borehole tensor strain measurements in Califorina, J. Geophys. Res., 92, 7981-7988, 1987.

Goulty, N.R., and R. Gilman, Repeated creep events on the San Andreas fault near Parkfield, California, recorded by a strainmeter array, J. Geophys. Res., 83, 5415-5419, 1978.

Gwyther, R.L., M.T. Gladwin, M. Mee, and R.H.G. Hart, Anomalous tensor strain at Parkfield during 1993-1994, Geophys. Res. Lett., 23, 2425- 2428, 1996.

Habermann, R.E., A test of two techniques for recognizing systematic errors in magnitude estimates using data from Parkfield, California, Bull. Seismol. Soc. Am., 76, 1660-1667, 1986.

Harris, R.A., and P. Segall, Detection of a Locked Zone at Depth on the Parkfield, California, Segment of the San Andreas Fault, J. of Geophys. Research, 92 (B8), 7945-7962, 1987.

Harris, R.A., and R.J. Archuleta, Slip budget and potential for M7 earthquake in Central California, Geophys. Res. Let., 15, 1215-1218, 1988.

Holzer, T.L., M.J. Bennett, T.L. Yound, and A.T.F. Chen, Parkfield, California, liquefaction prediction, Bull. Seismol. Soc. Am., 78, 385-389, 1988.

Isenberg,J., E. Richardson, and T.D. O'Rourke, Experiment on performance of buried pipelines across San Andreas fault, Tech. Rep. NCEER-89-0005, Natl. Center for Earthquake Eng. Res., State Univ. of N.Y. at Buffalo, March 10, 1989.

Johnson, P.A., and T.V. McEvilly, Parkfield seismicity: Fluid driven?, J. Geophys. Res., 100 (B7), 12,937-12,950, 1995a.

Johnston, M.J.S., A.T. Linde, M.T. Gladwin, and R.D. Borcherdt, Fault failure with moderate earthquakes, Tectonophysics, 144, 189-206, 1987.

Jones, L.M., Foreshocks (1966-1980) in the San Andreas system, Bull. Seismol. Soc. Am., 74, 1361-1380, 1984.

Jongmans, D., and P.E. Malin, Microearthquake S-wave observations from 0 to 1 km in the Varian well at Parkfield, California, Bull. Seismol. Soc. Am., 85, 1805-1820, 1995.

Kagan, Y.Y., Statistical aspects of Parkfield earthquake sequence and Parkfield prediction experiment, Tectonophysics, 270, 207-219, 1997.

Karageorgi, E., R. Clymer, and T.V. McEvilly, Seismological studies at Parkfield: II. Search for temporal variations in wave propagation using Vibroseis, Bull. Seismol. Soc. Am., 82, 1388 1415, 1992.

Karageorgi, E.D., T.V. McEvilly, and R.W. Clymer, Seismological studies at Parkfield IV: Variations in controlled-source waveform parameters and their correlation with seismic activity 1987-1994, Bull. Seismol. Soc. Am., 1996.

Kennedy, B.M., Y.K. Kharaka, W.C. Evans, A. Ellwood, D.J. DePaolo, J. Thordsen, G. Ambats, and R.H. Mariner, Mantle fluids in the San Andreas fault system, California, Science, 278, 1278-1281, 1997.

King, N.E., P. Segall, and W. Prescott, Geodetic measurements near Parkfield, California, J. Geophys. Res., 92, 2747-2766, 1987.

Korneev, V.A., T.V. McEvilly, and E.D. Karageorgi, Seismological studies at Parkfield VIII: Modeling the observed travel-time changes, Bull. Seismol. Soc. Am., 90 (3), 702-708, 2000.

Lachenbruch, A.H.a.J.H.S., Heat flow and energetics of the San Andreas fault zone, J. Geophys. Res., 85 (B11), 6185-6222, 1980.

Langbein, J., R. Gwyther, R. Hart, and M.T. Gladwin, Slip rate increase at Parkfield in 1993 detected by high-precision EDM and borehole tensor strainmeters, Geophys. Res. Lett., 26, 2529 2532, 1999.

Langbein, J.O., R.O. Burford, and L.E. Slater, Variations in fault slip and strain accumulation at Parkfield, California: Initial results using two-color geodimeter measurements, 1984-1988, J. Geophys. Res., 95, 2533-2552, 1990.

Langbein, J., E. Quilty, K. Breckenridge, Sensitivity of crustal deformation instruments to changes in secular rate. Geophys. Res. Let., 20, 85-88, 1993.

Langbein, J.O., Earthquake explanations, Nature, 349, 287., 1991.

Leary, P., A 200 m wide fault zone low velocity layer on the San Andreas fault at Parkfield: Results from analytic waveform fits to trapped wave groups, Seismol. Res. Lett., 63 (1), 62, 1992.

Lees, J.M., and P.E. Malin, Tomographic images of P wave velocity variation at Parkfield, California, J. Geophys. Res., 95, 21,793-21,804, 1990.

Lewicki, J.L., and S.L. Brantley, CO_2 degassing along the San Andreas fault, Parkfield, California, Geophys. Res. Lett., 27 (1), 5-8, 2000.

Lienkaemper, J.J., and W.H. Prescott, Historic surface slip along the San Andreas fault near Parkfield, California, J. Geophys. Res., 94, 17,647-17,670, 1989.

Lindh, A.G., and D.M. Boore, Control of rupture by fault geometry during the 1966 Parkfield earthquake, Bull. Seismol. Soc. Am., 71, 95-116, 1983.

Louie, J.N., R.W. Clayton, and R.J. LeBras, Three-dimensional imaging of steeply dipping structures near the San Andreas fault, Parkfield, California, Geophysics, 53, 176-185, 1988.

Lorenzetti, E.A. and T.E. Tullis, Geodetic predictions of a strike-slip fault model; implications of intermediate and short-term earthquake predition, J. Geophys. Res., 94, 12343-12361, 1989.

Malin, P.E., and M.G. Alvarez, Stress diffusion along the San Andreas fault at Parkfield, California, Science, 256, 1005-1007, 1992.

Malin, P.E., S.N. Blakeslee, M.G. Alvarez, and A.J. Martin, Microearthquake imaging of the Parkfield asperity, Science, 244, 557-559, 1989.

McBride, J.H., and L.D. Brown, Reanalysis of the COCORP deep seismic reflection profile across the San Andreas fault, Parkfield, California, Bull. Seismol. Soc. Am., 76, 1668-1686, 1986.

McEvilly, T.V., Earthquakes near Parkfield, California: Comparing the 1934 and the 1966 Sequences, Science, 205, 1375-1377, 1979.

McEvilly, T.V., W.H. Bakun, and K.B. Casaday, The Parkfield, California earthquakes of 1966, Bull. Seismol. Soc. Am., 57, 1221-1244, 1967.

McGill, P.R., A.C. Fraser-Smith, and R.A. Helliwell, Ultra-low frequency magnetic field measurements at Parkfield, California, during the Level-A and Level-B earthquake alerts of October, 1992, Supplement to EOS, Trans. Am. Geophys. Union, 74, 379, 1993.

McJunkin, R.D., and A.F. Shakal, The Parkfield strong-motion array, California Geology, 36, 27-34, 1983.

Meltzner, A.J., and Wald, D.J., Bull. Seismol. Soc. Am. 89, 1109-1120, 1999.

Michael, A.J, and D. Eberhart-Phillips, Relationships between fault behavior, subsurface geology, and three-dimensional velocity models, Science, 253, 651-654, 1991

Michael, A.J., and L.M. Jones, Seismic alert probabilities at Parkfield, California, revisited, Bull. Seismol. Soc. Am., 88 (1), 117-130, 1998.

Michael, A.J., and J. Langbein, Earthquake predictions lessons from Parkfield experiment, EOS, Trans., Amer. Geophys. Un., 74, 153-155, 1993

Michelini, A., and T.V. McEvilly, Seismological studies at Parkfield: I. Simultaneous inversion for velocity structure and hypocenters using B-splines parameterization, Bull. Seismol. Soc. Am., 81, 524-552, 1991.

Miller, S.A., Fluid-mediated influence of adjacent thrusting on the seismic cycle at Parkfield, Nature, 382, 799-802, 1996.

Murray, J.R., P. Segall, Geophys. Res. Let., 2001,

Nishenko, S.P., and R. Buland, A generic recurrence interval distribution for earthquake forecasting, Bull. Seismol. Soc. Am., 77, 1382-1399, 1987.

Nadeau, R., M. M. Antolik, P. Johnson, W. Foxall, and T.V. McEvilly, Seismological studies at Parkfield III: Microearthquake clusters in the study of fault-zone dynamics, Bull. Seismol. Soc. Am., 84, 247-263, 1994.

Nadeau, R.M., A search for temporal changes in travel times and polarization at parkfield using earthquake sources, Seismol. Research Letters, 63 (1), 62, 1992.

Nadeau, R.M., and T.V. McEvilly, Characteristic microearthquake response to the December 20, 1994 M5 event at Parkfield, CA: Changes in recurrence interval and fault slip rate, Seis. Res. Lett., 68, 325, 1997a.

Nadeau, R.M., and T.V. McEvilly, Seismological studies at Parkfield V: Characteristic microearthquake sequences as fault-zone drilling targets, Bull. Seismol. Soc. Am., 87 (6), 1463 1472, 1997b.

Nason, R.D., F.R. Philippsborn, and P.A. Yamashita, Catalog of creepmeter measurements in central California from 1968 to 1972, U.S. Geological Survey, Menlo Park, Calif., 1974.

National Earthquake Prediction Evaluation Working Group, Earthquake Research at Parkfield, California, for 1993 and beyond, U.S. Geological Survey Circular 1116, 14pp., 1994.

Nishioka, G.K., and A.J. Michael, A detailed seismicity study of the Middle Mountain zone at Parkfield, California, Bull. Seismol. Soc. Am., 80, 577-588, 1990.

Noguchi,. M. and H. Wakita, A method for continuous measurement of radon in groundwater for earthquake prediction, J. Geophys. Res., 82, 1353-1357, 1977.

O'Neill, M.E., Source dimensions and stress drops of small earthquakes near Parkfield, California, 74, 27-40, 1984.

Park, S.K., Monitoring resistivity changes prior to earthquakes in Parkfield, California, with telluric arrays, J. Geophys. Res., 96, 14,211-14,237, 1991.

Park, S.K., Monitoring resistivity changes in Parkfield, California: 1988-1995, J. Geophys. Res., 102 (B11), 24,545-24,559, 1997.

Park, S.K., and D.V. Fitterman, Sensitivity of the telluric monitoring array in Parkfield, California to changes of resistivity, J. Geophys. Res., 95, 15,557-15,571, 1990.

Parkfield Working Group, Parkfield, First short-term earthquake warning, EOS, Trans., Amer. Geophys. Un., 74, 152-153, 1993.

PBO Steering committee, The Plate Boundary Observatory; Creating a four-dimensional image of the deformation of Western North America, http://www.unavco.ucar.edu/community/publications/proposals/PBOwhitepaper.pdf, 2000.

Poley, C.M., A.G. Lindh, W.H. Bakun, and S.S. Schulz, Temporal changes in microseismicity and creep near Parkfield, California, Nature, 327, 134- 137, 1987.

Quilty, E., and E. Roeloffs, Water level changes in response to the December 20, 1994 M4.7 earthquake near Parkfield, California, Bull. Seismol. Soc. Am., 87 (2), 310-317, 1997.

Quilty, E.G., and E.A. Roeloffs, Coseismic water level changes in wells near Parkfield, California, in response to a magnitude 5.0 earthquake on December 20, 1994, EOS, Trans. Am. Geophys. Union/Supplement, 76 (46), F150, 1995.

Roeloffs, E., Persistent water level changes in a well near Parkfield, California, due to local and distant earthquakes, J. Geophys. Res., 103 (B1), 869-889, 1998.

Roeloffs, E., Creep rate changes at Parkfield, California 1966-1999: Seasonal, Precipitation Induced, and Tectonic, J. Geophys. Res., submitted, 2000b.

Roeloffs, E., and J. Langbein, The earthquake prediction experiment at Parkfield, California, Reviews of Geophysics, 32 (3), 315-336, 1994.

Roeloffs, E., and E. Quilty, Water level and strain changes preceding and following the August 4, 1985 Kettleman Hills, California, Earthquake, Pure Appl. Geophys., 149, 21-60, 1997.

Roeloffs, E.A., S.S. Burford, F.S. Riley, and A.W. Records, Hydrologic effects on water level changes associated with episodic fault creep near Parkfield, California, J. Geophys. Res., 94 (B9), 12,387-12,402, 1989.

Roeloffs, E., The Parkfield, California, Earthquake Experiment: An update in 2000., Current Science, 79, 1226-1236, 2000.

Rudnicki, J.W., J. Yin, and E. Roeloffs, Analysis of water level changes induced by fault creep at Parkfield, California, J. Geophys. Res., 98, 8143-8152, 1993.

Sass, J.A., S.P. Galanis, C.F. Williams, A.H. Lachenbruch, and F.V. Grubb, Thermal regime of the San Andreas fault near Parkfield, California, (submitted), 1996.

Sato, M., A.J. Sutton, K.A. McGee, and S. Russell-Robinson, Monitoring of hydrogen along the San Andreas and Calaveras faults in central Califorina in 1980-1984, J. Geophys. Res., 91, 12315-12326, 1986.

Savage, J.C., The Parkfield prediction fallacy, Bull. Seismol. Soc. Am., 83, 1-6, 1993.

Savage, J.C., and R.O. Burford, Geodetic determination of relative plate motion in central California, J. Geophys. Res. 78, 832-845, 1973.

Schulz, S.S., Catalog of creep meter measurements in California from 1966 through 1988, U.S. Geol. Surv. Open File Rep., 89-650, 1989.

Segall, P., and Y. Du, How similar were the 1934 and 1966 Parkfield earthquakes?, J. Geophys. Res., 98, 4527-4538, 1993.

Segall, P., and R. Harris, Slip deficit on the San Andreas fault at Parkfield, California, as revealed by inversion of geodetic data, Science, 233, 1409-1413, 1986.

Segall, P., and R. Harris, Earthquake deformation cycle on the San Andreas fault near Parkfield, California, J. Geophys. Res., 92, 10,511-10,525, 1987.

Shedlock, K.M., T.M. Brocker, and S.T. Harding, Shallow structure and deformation along the San Andreas faults in Cholame Valley, California, based on high-resolution reflection profiling, J. Geophys. Res., 95, 5003-5020, 1990.

Sieh, K.E., Slip along the San Andreas fault associated with the great 1857 earthquake. Bull. Seismol. Soc. Am., 68, 1421-1428, 1978a

Sieh, K.E., Central California foreshocks of the great 1857 earthquake. Bull. Seismol. Soc. Am., 68, 1731-1749, 1978b

Silverman, S., C. Mortensen, and M. Johnston, A satellite-based digital system for low-frequency geophysical data., Bull. Seismol. Soc. Am., 79, 189-198, 1989.

Simpson, R.W., S.S. Schulz, L.D. Dietz, and R.O Burford, The response of the creeping parts of the San Andreas fault to earthquakes o nearby faults: Two examples, Pure Appl. Geophys., 126, 665-685, 1988.

Simpson, R.W., R.C. Jachens, and C.R. Wentworth, Average topography, isostatic residual gravity, and aeromagnetic maps of the the Parkfield region, U.S. Geological Survey Open-File Report, 89-13, 1989.

Sims, J.D., Chronology of displacement on the San Andreas fault in central California: Evidence from reversed positions of exotic rock bodies near Parkfield, California, U.S. Geological Survey Open-File Report, 89-571, 1989.

Sims, J.D., Geologic map of the San Andreas fault in the Parkfield 7.5-minute quadrangle, Monterey and Fresno counties, California, U.S. Geological Survey Miscellaneous Field Studies, Map MF-2115, 1990.

Sims, J.D., Chronology of displacement on the San Andreas fault in central California: Evidence from reversed positions of exotic rock bodies near Parkfield, California, Geol. Soc. Am. Memoire, 178, 231-256, 1993.

Slawson, W.F. and J.C. Savage, Deformation near the junction of the creeping and locked segments of the San Andreas Fault, Cholame Valley, California (1970-1980), Bull. Seismol. Soc. Am., 73, 140701414, 1983.

Smith, S.W., and M. Wyss, Displacement of the San Andreas fault subsequent to the 1966 Parkfield earthquake, Bull. Seismol. Soc. Am., 58, 1955-1973, 1968.

Spudich, P., L.K. Steck, M. Hellweg, J.B. Fletcher, and L.M. Baker, Transient stresses at Parkfield, California, produced by the M7.4 Landers earthquake of June 28, 1992: Observations from the UPSAR dense seismograph array, J. Geophys. Res., 100 (B1), 675-690, 1995.

Stewart, M., and M.J.S. Johnston, Bulk and shear moduli of near-surface geologic units near the San Andreas fault at Parkfield, California, U.S. Geological Survey Open-File Report, 93-538, 1993.

Stuart, W.D., Seismic quiescence at Parkfield due to detachment faulting, Nature, 349, 58-61, 1991.

Stuart, W.D., Theoretical models for faulting and ground deformation at Parkfield, California, EOS, Trans. Am. Geophys. Union, Supplement (78), S220, 1997.

Stuart, W.D., R.J. Archuleta, and A.G. Lindh, Forecast model for moderate earthquakes near Parkfield, California, J. Geophys. Res., 90, 592-604, 1985.

Stuart, W.D., and T.E. Tullis, Fault model for preseismic deformation at Parkfield, California, J. Geophys. Res., 100 (B12), 24,079-24,099, 1995.

Stuart, W.D., P.O. Banks, Y. Sasai, and S.-W. Liu, Piezomagnetic field for Parkfield fault model, J. Geophys. Res., 100, 24101-24110, 1995.

Sylvester, A.G., Nearfield vertical displacement in the creeping segment of the San Andreas fault, central California, 1975-1994, Tectonophysics, 247, 25-47, 1995.

Thatcher, W., Systematic inversion of geodetic data in central California, J. Geophys. Res., 84, 2283-2295, 1979.

Thompson, J.M., and L.D. White, Chemical analyses of water from the GTA-1 well, Parkfield, California, and other nearby spring and well waters, U.S. Geological Survey Open-File Report, 91-0003, 1991.

Toda, S., and R.S. Stein, Response of the San Andreas Fault to the 1983 Coalinga-Nunez Earthquakes: An application of interaction-based probabilities for Parkfield, Submitted, J. Geophys. Res, 2001.

Toppozada, T.R., C. Hallstrom, and D. Ransom, M ¿ 5.5 earthquakes within 100 km of Parkfield, California, Seismol. Res. Lett., 61, 42, 1990.

Tullis, T., Rock friction and its implications for earthquake prediction examined via models of Parkfield earthquakes, Proc. Natl. Acad. Sci., 93, 3803-3810, 1996.

Unsworth, M.J., P.E. Malin, G.D. Egbert, and J.R. Booker, Internal structure of the San Andreas fault at Parkfield, California, Geology, 25 (4), 359-362, 1997.

Wyss, M., Changes of mean magnitude of Parkfield seismicity: a part of the precursory process?, Geophys. Res. Lett., 17, 2429-2432, 1990.

Wyss, M., Increased mean depth of earthquakes at Parkfield, Geophys. Res. Lett., 18, 617-620, 1991.

Wyss, M., P. Bodin, and R.E. Habermann, Seismic quiescence at Parkfield: An independent indication of an imminent earthquake, Nature, 345, 426-428, 1990a.

Wyss, M., L. Slater, and R.O. Burford, Decrease in deformation rate as a possible precursor to the next Parkfield earthquake, Nature, 345, 428-431, 1990b.

Zoback, M.D., Hickman, S.H., and Ellsworth, W.L., Scientific Drilling into the San Andreas Fault at Parkfield, CA: Project overview and operation; Proposal prepared for the National Science Foundation, http://pangea.Stanford.EDU/∼zoback/FZD/, 1998.

Table. Monitoring Instruments

Network	Number of sites	Sensitivity	Measurement Interval	Status	References
Seismicity (NCSN)	40	$M \geq 1.0$	continuous	on line	*Nishioka and Michael* [1990]
Continuous dilational strain	7	10^-9^2	10 min	4 sites working	*Myren and Johnston* [1989]
Continuous tensor strain	3	10^-9^2	15 min	on line	*Gladwin et al.* [1987]
Magnetic field	7	0.25 nT	10 min	on line	*Mueller et al.* [1994]
Creepmeter	12	0.05 mm[2]	10 min	sensitive to rain	*Schulz* [1989]
Ground water level	10	1 mm	15 min	7 sites working	*Roeloffs et al.* [1989]
Two-color EDM	18 lines	1 mm	3/week	operated once every 3 weeks[1]	*Langbein et al.* [1990]
Tilt	5	1 μ rad	10 min	discontinued	*Mortensen et al.* [1978]
Groundwater radon	2	1 pCi/L	10 min	discontinued	*Noguichi and Wakita* [1978]
Soil Hydrogen	7	10 ppm	10 min	discontinued	*Sata et al.* [1986]
Resistivity	6 dipoles	1%	daily average	on line	*Park* [1991]
Ultra-low Frequency Magnetic field	2	1 pT	30 min average	merged with E-M exp.	*McGill et al.* [1993]
E-M Field	3 mag. 2 electric				*Morrison ???*
Continuous GPS	6	2 mm	1-day average	8 more in 2001	Langbein *Oral comm.* [2001]
Campaign GPS	34	3 mm	1 every 3 years	last measured 1996 Replaces Trilateration	Langbein *Oral comm.* [2001] *King et al.* [1987]
Leveling	7 lines	1 mm/km	infrequent		*Sylvester* [1991]

[1] To be replaced by GPS

[2] The sensitivity is appropriate for 24 hours or less. Because of increasing noise at longer periods, signal must be larger to be detected at longer period *Langbein et al.* [1993].

Table. Monitoring Instruments

Network	Number of sites	Sensitivity	Measurement Interval	Status	References
HRSN Borehole Seismic network	10	$M \geq -1$	continuous	3 more 2001	*Michelini et*
Viborseis waveform	80 paths	5 ms	4/year	discontinued	*Current Ref?*
UPSAR Dense Seismic Array	14 geophone 14 accelerometers in $1km^2$ area	$M \geq 3$	continuous	on line	*Fletcher el al*
EPRI Dense Seismic Array	21 FBA in 120 meter radius		continuous	discontinued	*Schneider el*
Liquefaction Array	5 accelerometers 7 piezometers			discontinued	*Holzer el al.*
CDMG Strong motion array	48 3-component SMA	$M \geq 4$	triggered	on line	*McJunkin an*
GEOS digital recording (acceleration, velocity and volume strain)	13 3-comp. FBA 7 geophones 6 strainmeters		triggered	operational	*Borcheerdt et*
Rupture Video camera	2 cameras	$M \geq 4$	triggered	operational	
Pipeline					disco
Turkey Flat Strong motion array	6 3-comp FBA 2 downhole 2 km linear array		triggered	operational	*Real and Tuc*

[1] To be replaced by GPS

[2] The sensitivity is appropriate for 24 hours or less. Because of increasing noise at longer periods, signal must be larger to be detected at longer period *Langbein et al.* [1993].

Figure Captions

Figure 1. Map showing 1966 epicenter, the surface trace of the San Andreas fault, the proposed SAFOD location, and instrument locations. Figure 1a shows the regional distribution of instrument networks and the locations of state and federal roads. Figure 1b shows the locations of instruments near Middle Mountain and near the town of Parkfield.

Figure 2. Pie charts showing the money spent at Parkfield.

Figure 3. Distribution of slip both in cross section on the San Andreas fault and in time. These results were derived by *Nadeau et al.* [1999] from repeating, micro-earthquakes at Parkfield. The top left panel shows the average, annual slip rate from recurrence intervals compared with surface measurements of slip. The white triangles are locations of repeating micro earthquakes, the white ellipses are the locations of the 4, $M > 4$ earthquake at Parkfield since 1986, and the brown square is the location of the 1966 $M6$ Parkfield earthquake. The color intensity is keyed to confidence limits for the slip rates. The right panel shows the spatial distribution of slip-rate changes in 6-month intervals. The rate changes are relative to 10/89. The bottom left panel show slip-rates derived from repeating earthquakes and independently from 2-color EDM measurements.

Figure 4. Examples of data from 15 years on monitoring deformation and seismicity. Figure 4a shows that statistics of Parkfield seismicity, data from a few of the creepmeters, and data from the two-color EDM network. The seismicity plot is for the Parkfield region. The black line is the cumulative number of $M > 1.7$ events since 1986. The red line is the cumulative moment; most of the moment release occured during the 1992-1994 interval. The creepmeter data for 5 sites are shown. The data have had their secular rates removed prior to plotting. The rates are identified next to each trace. The red traces are the residual data but the black traces have had signals, with frequencies between 0.5 and 1.5 cycles per year, removed. Note that the amplitude of the annual periodicity is more than 5 mm peak to peak for some of the creepmeters which has been removed by filtering. The top plot shows changes in length of 4, EDM baselines. The data have had their secular rates removed. These baselines form two pairs where the reflector monuments are separated by 30 meters. For the data shown in red, the monument is a shallow monument similar to those used at creepmeters. For the data shown in black, the monument is a deeply braced monument described by *Langbein et al.* [1995]. Note that the data from the braced monuments are not contaminated by a seasonal signal. In Figure 4b, detailed records of creep and strain changes are seen for a creep event that occurred in September 2000. The fault creep data are shown in black and the strain changes from the borehole strainmeter network are shown in colors. Included are both strain data from the dilatometers and the tensor strain meters. Detectable strain changes were recorded at both the FR and ED tensor strainmeters. A corresponding change in dilatation was recorded at FR.

Figure 5. Results of fitting a model of fault slip and strain accumulation to the two-color EDM data. The strain changes inferred from the EDM data are compared with strain changes recorded at two of the borehole tensor strainmeters. The time-dependent model consists of estimating the temporal changes for six parameters. Fault slip is represented by simple, rigid-block motion on the San Andreas fault. In addition, since the central monument at Carr may move independent of tectonic changes, the two components of displacement of this monument are estimated. Finally, since the actual spatial distribution of slip is more complex than simple, uniform slip, the three components of the strain tensor are also modeled to simulate part of the complexity. The results from the EDM derived model have had a linear-in-time trend removed from the results using the 1986 to 1992 interval.

Figure 6. A cross section of the fault zone looking along strike from the southwest. The proposed drilling for the SAFOD experiment is shown superimposed over the resisitivety structure from *Unsworth et al.* [1997] and the locations of nearby earthquakes.

Parkfield Monitoring Sites

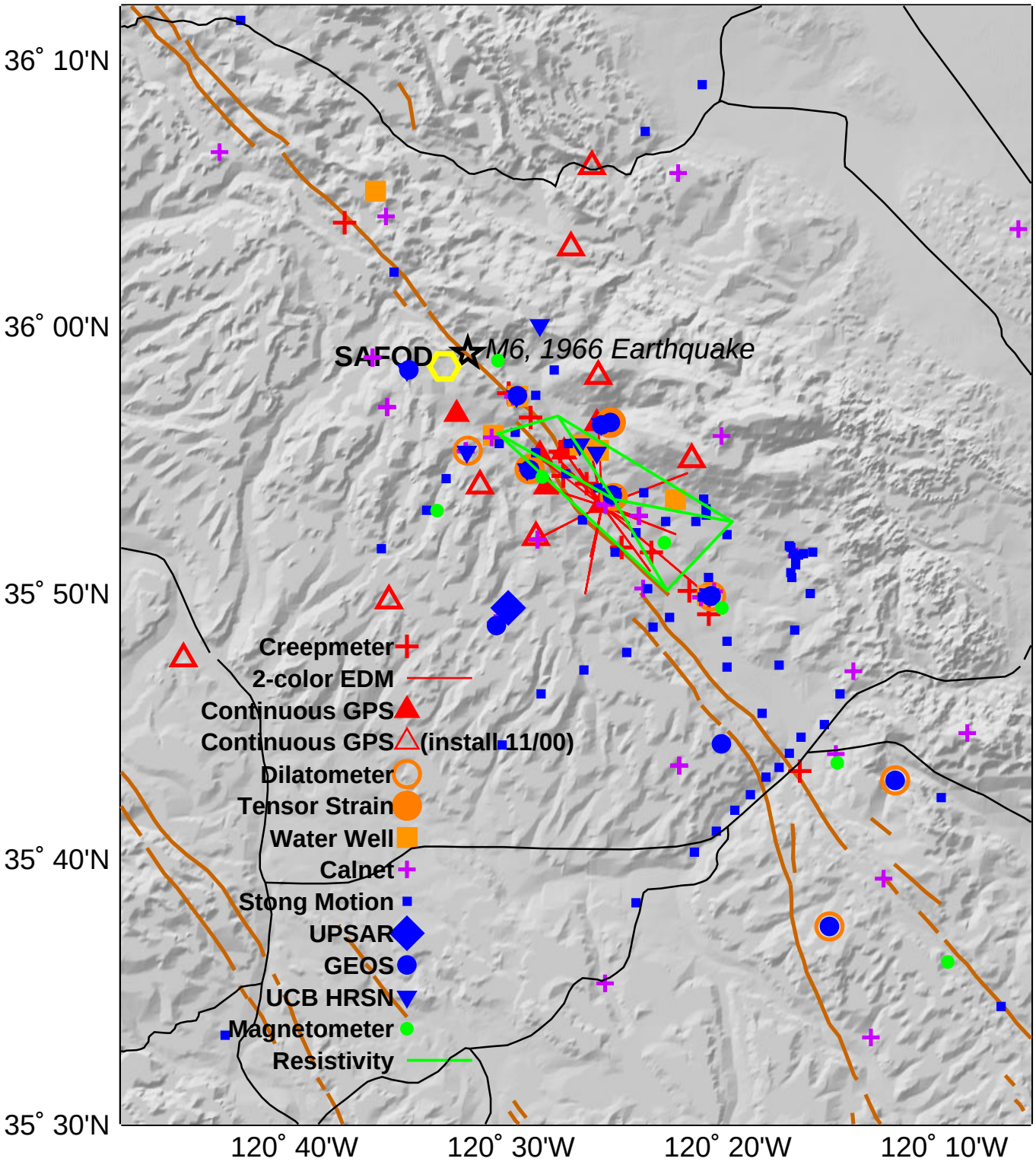

Figure 1a

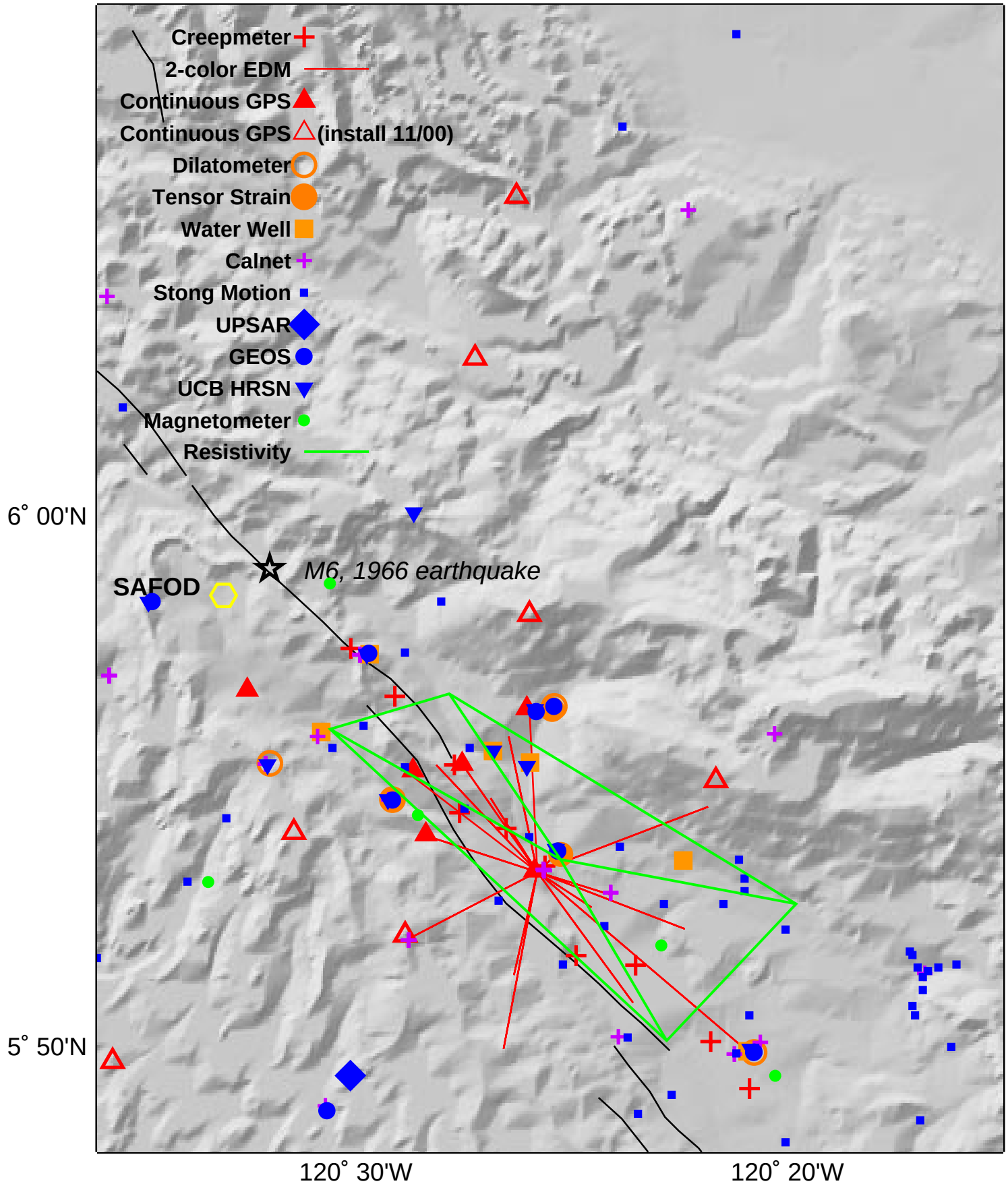
Creepmeter
2-color EDM
Continuous GPS
Continuous GPS (install 11/00)
Dilatometer
Tensor Strain
Water Well
Calnet
Stong Motion
UPSAR
GEOS
UCB HRSN
Magnetometer
Resistivity
M6, 1966 earthquake
SAFOD
6˚ 00'N
5˚ 50'N
120˚ 30'W
120˚ 20'W

Figure 1b

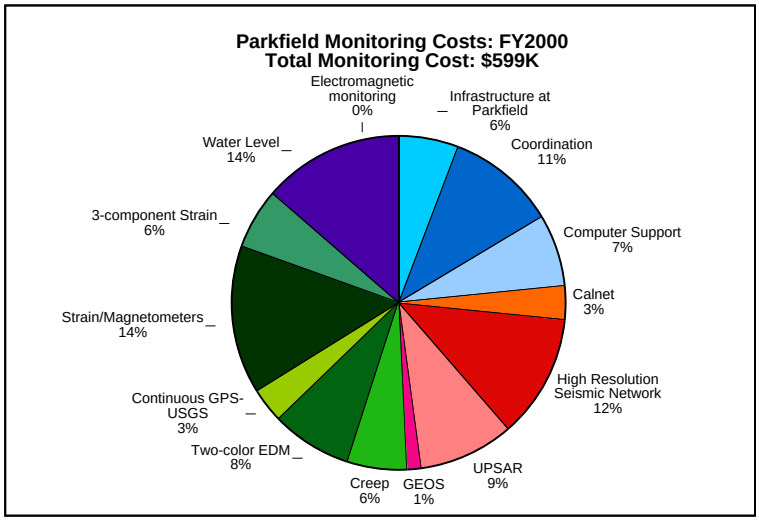
Parkfield Monitoring Costs: FY2000
Total Monitoring Cost: $599K
Electromagnetic monitoring 0%
Infrastructure at Parkfield 6%
Coordination 11%
Computer Support 7%
Calnet 3%
High Resolution Seismic Network 12%
UPSAR 9%
GEOS 1%
Creep 6%
Two-color EDM 8%
Continuous GPS-USGS 3%
Strain/Magnetometers 14%
3-component Strain 6%
Water Level 14%

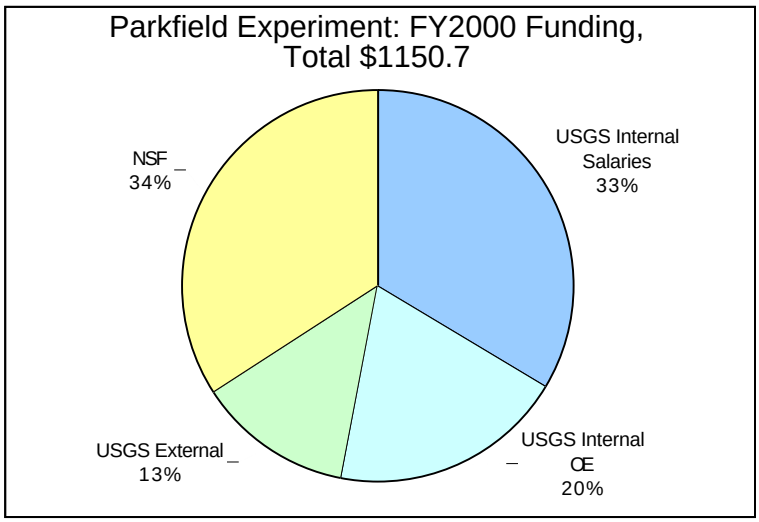
Parkfield Experiment: FY2000 Funding,
Total $1150.7
USGS Internal Salaries 33%
USGS Internal OE 20%
USGS External 13%
NSF 34%

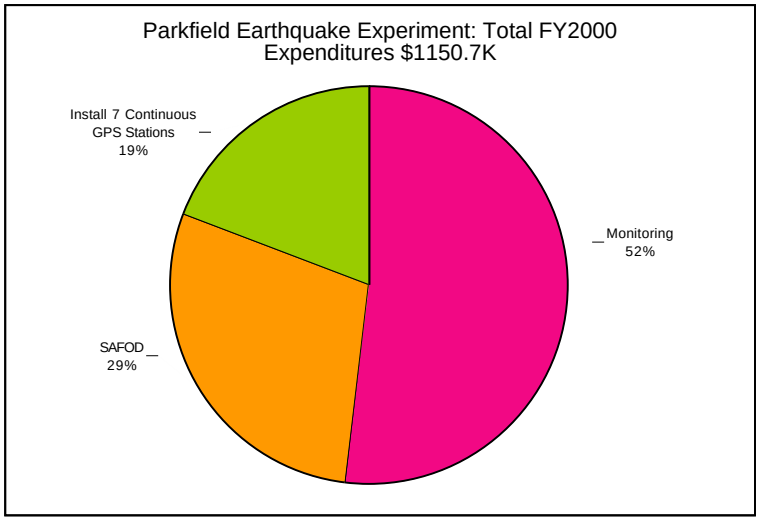
Parkfield Earthquake Experiment: Total FY2000
Expenditures $1150.7K
Monitoring 52%
SAFOD 29%
Install 7 Continuous GPS Stations 19%

Figure 2

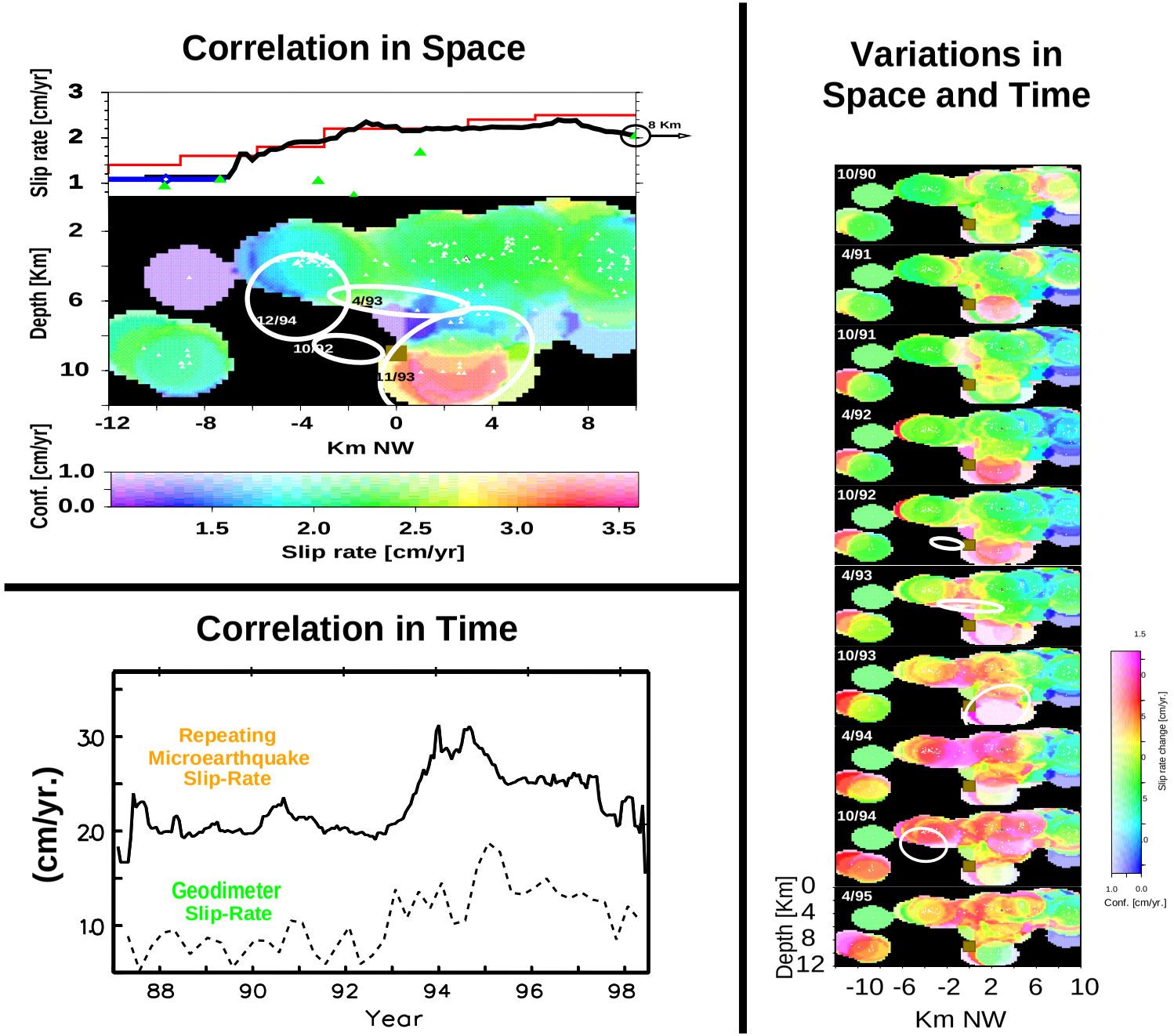
Correlation in Space
Slip rate [cm/yr]
3
2
1
8 Km
Depth [Km]
2
6
10
4/93
12/94
10/92
11/93
-12
-8
-4
0
4
8
Km NW
Conf. [cm/yr]
1.0
0.0
1.5
2.0
2.5
3.0
3.5
Slip rate [cm/yr]
Correlation in Time
(cm/yr.)
3.0
2.0
1.0
Repeating
Microearthquake
Slip-Rate
Geodimeter
Slip-Rate
88
90
92
94
96
98
Year
Variations in
Space and Time
10/90
4/91
10/91
4/92
10/92
4/93
10/93
4/94
10/94
4/95
Depth [Km]
0
4
8
12
-10
-6
-2
2
6
10
Km NW
1.5
0.0
Slip rate change [cm/yr.]
1.0
0.0
Conf. [cm/yr.]

Figure 3

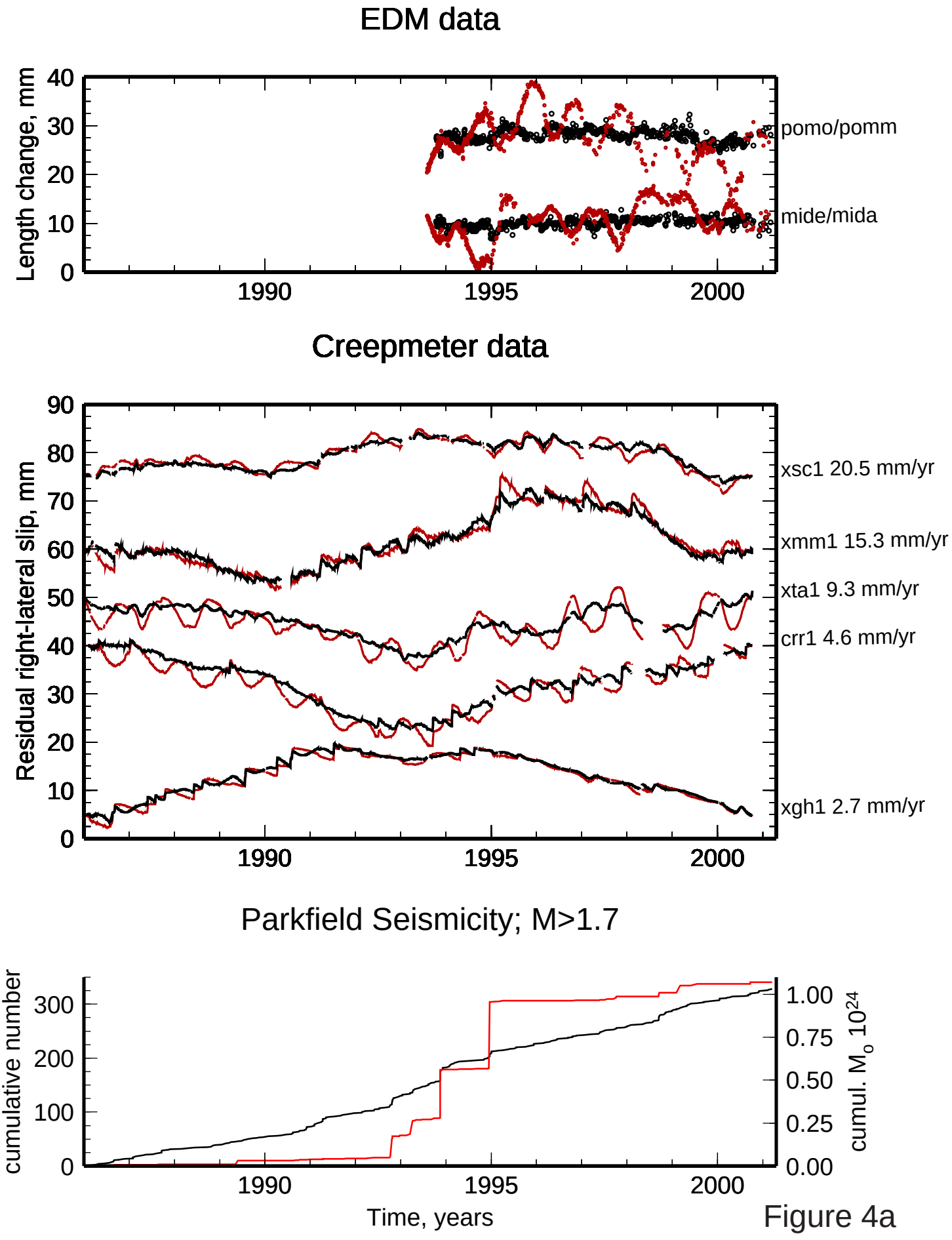
EDM data
Length change, mm
40
30
20
10
0
1990
1995
2000
pomo/pomm
mide/mida
Creepmeter data
Residual right-lateral slip, mm
90
80
70
60
50
40
30
20
10
0
1990
1995
2000
xsc1 20.5 mm/yr
xmm1 15.3 mm/yr
xta1 9.3 mm/yr
crr1 4.6 mm/yr
xgh1 2.7 mm/yr
Parkfield Seismicity; M>1.7
cumulative number
300
200
100
0
1990
1995
2000
Time, years
1.00
0.75
0.50
0.25
0.00
cumul. M0 10^24

Figure 4a

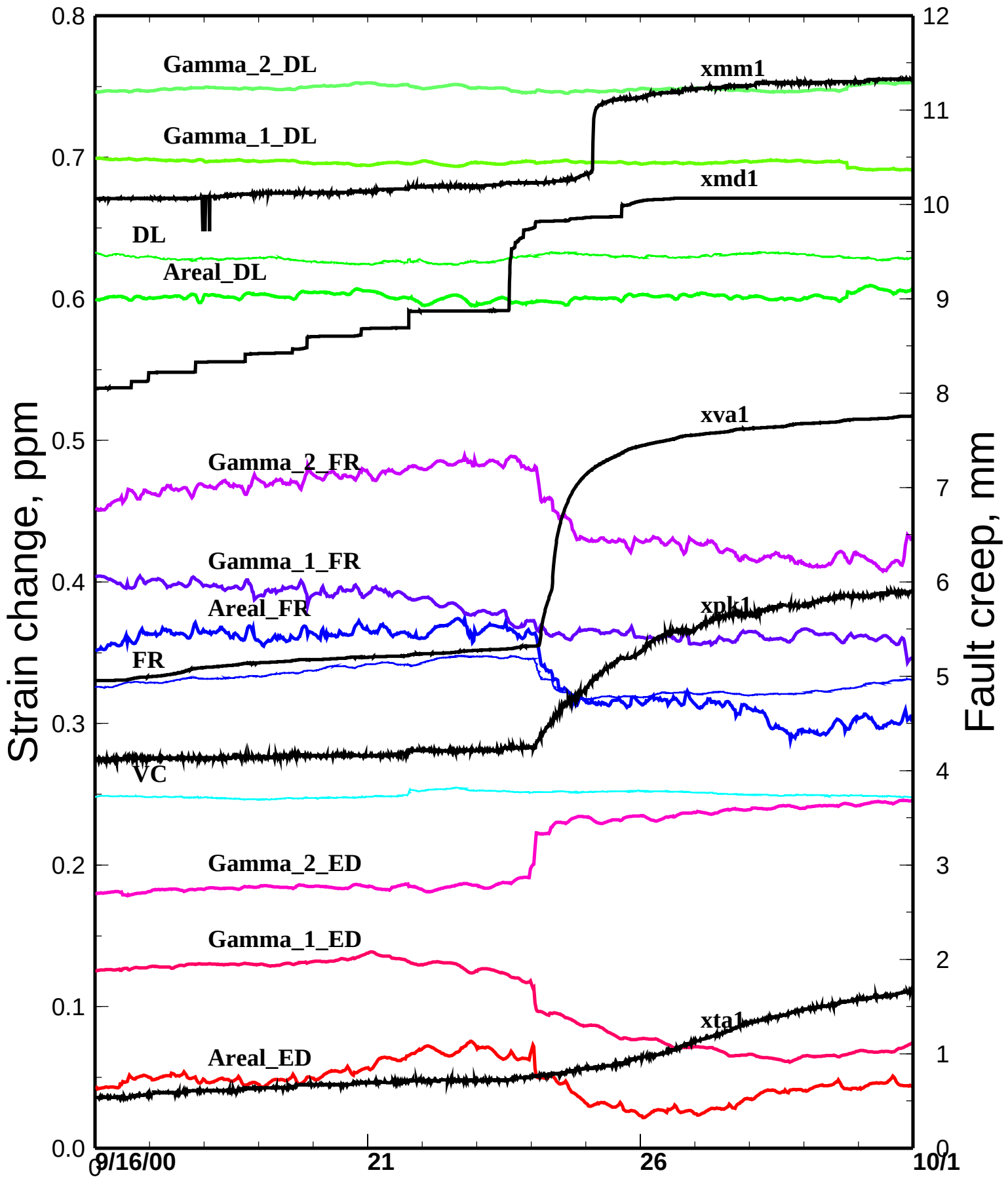
Sept 2000 Parkfield event
Strain change, ppm
Fault creep, mm
0.8
0.7
0.6
0.5
0.4
0.3
0.2
0.1
0.0
12
11
10
9
8
7
6
5
4
3
2
1
0
9/16/00
21
26
10/1
Gamma_2_DL
Gamma_1_DL
DL
Areal_DL
Gamma_2_FR
Gamma_1_FR
Areal_FR
FR
VC
Gamma_2_ED
Gamma_1_ED
Areal_ED
xmm1
xmd1
xva1
xpk1
xta1

Figure 4b

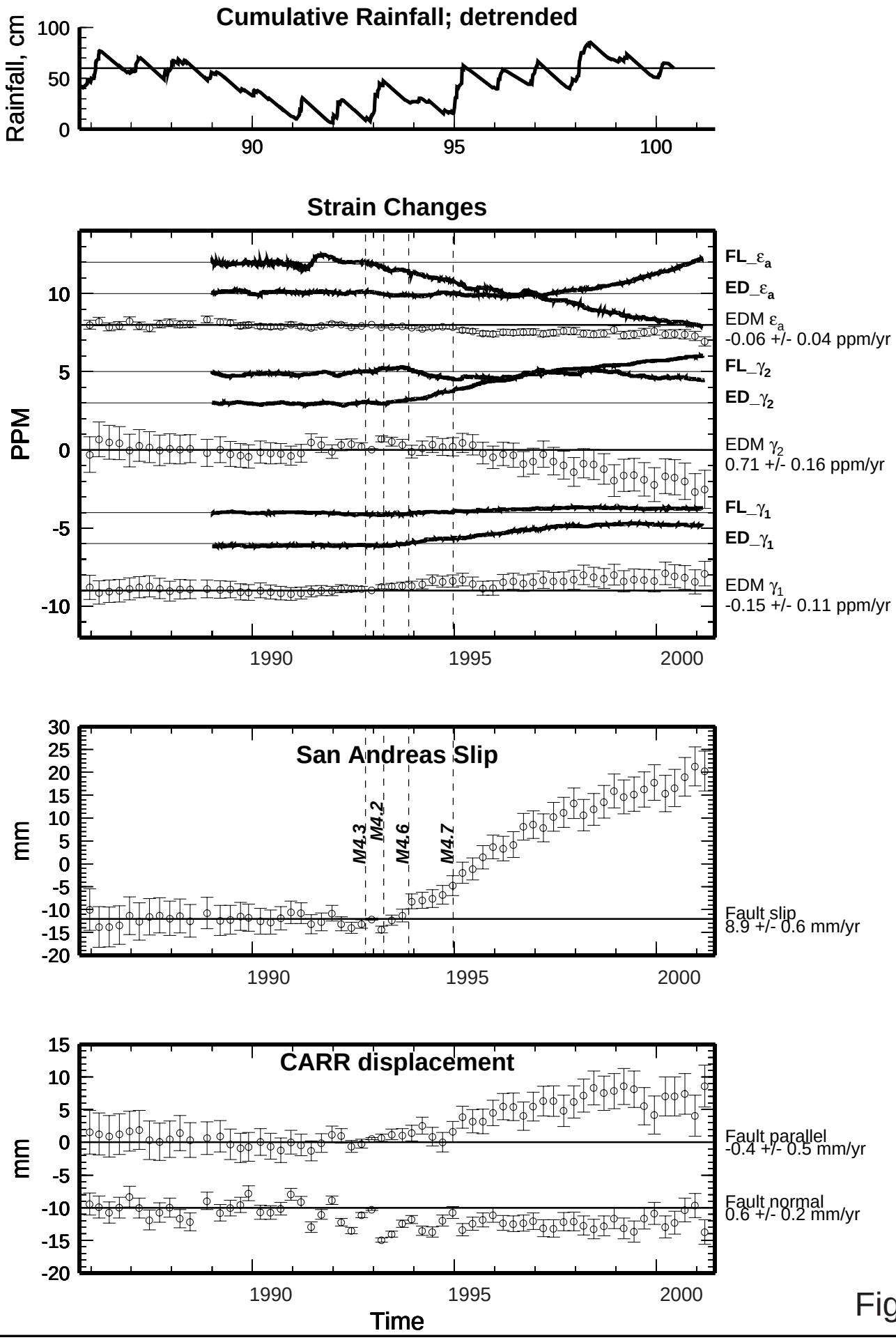
Cumulative Rainfall; detrended
Rainfall, cm
100
50
0
90
95
100
Strain Changes
PPM
10
5
0
-5
-10
1990
1995
2000
FL_εa
ED_εa
EDM εa
-0.06 +/- 0.04 ppm/yr
FL_γ2
ED_γ2
EDM γ2
0.71 +/- 0.16 ppm/yr
FL_γ1
ED_γ1
EDM γ1
-0.15 +/- 0.11 ppm/yr
San Andreas Slip
mm
30
25
20
15
10
5
0
-5
-10
-15
-20
M4.3
M4.2
M4.6
M4.7
1990
1995
2000
Fault slip
8.9 +/- 0.6 mm/yr
CARR displacement
mm
15
10
5
0
-5
-10
-15
-20
1990
1995
2000
Time
Fault parallel
-0.4 +/- 0.5 mm/yr
Fault normal
0.6 +/- 0.2 mm/yr

Figure 5

Proposed SAFOD experiment
and
Resistivity Profile

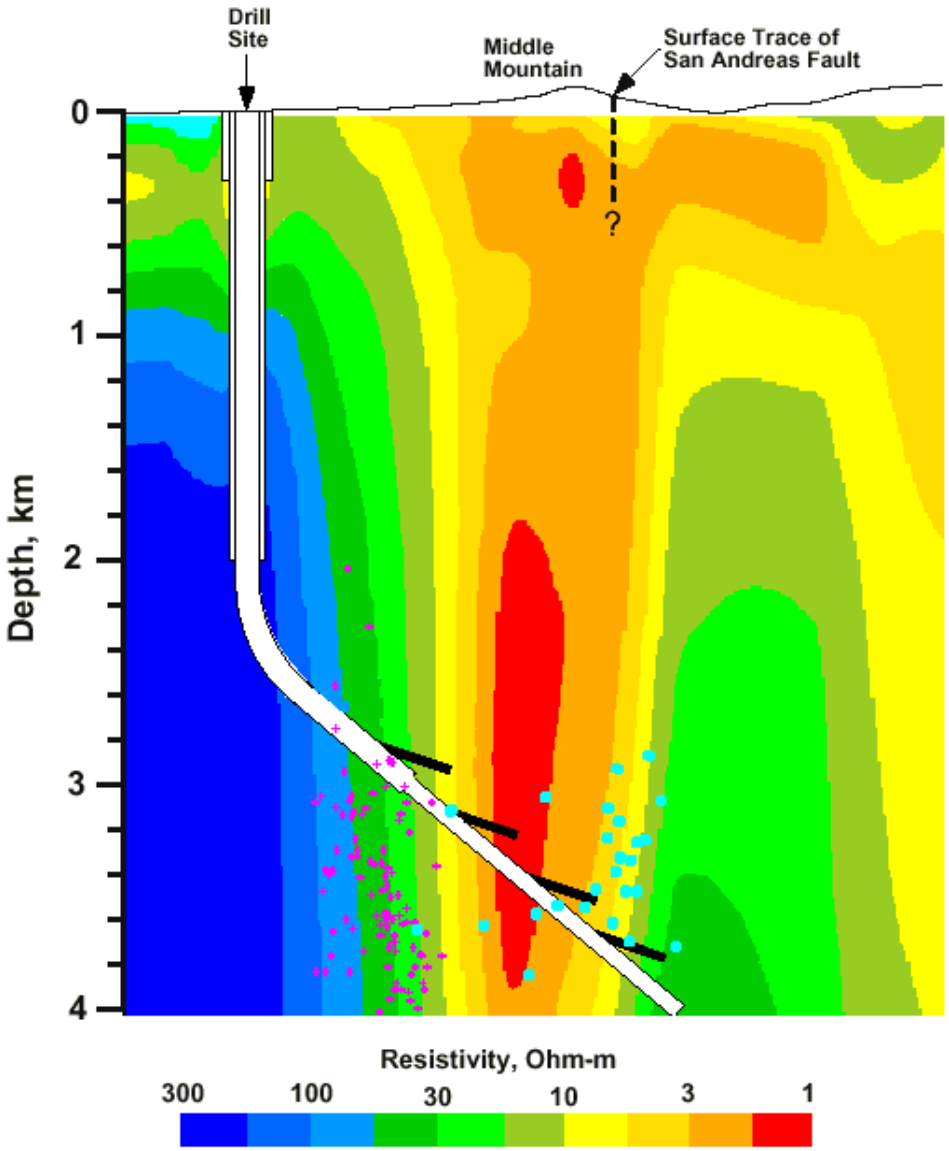

Figure 6